THE ASTROPHYSICAL JOURNAL, 291:755–771, 1985 April 15

FAR-INFRARED SPECTROSCOPY OF GALAXIES: THE 158 MICRON C^+ LINE AND THE ENERGY BALANCE OF MOLECULAR CLOUDS

M. K. CRAWFORD,[1] R. GENZEL,[1] C. H. TOWNES,[1] AND DAN M. WATSON[2]

Received 1984 July 26; accepted 1984 October 31

ABSTRACT

We have detected the 158 μm ground-state fine-structure line of singly ionized carbon in six gas-rich galaxies and mapped its spatial distribution in M82, NGC 1068, and M83. The [C II] line is bright toward the centers of all observed galaxies, containing about 0.5% of the bolometric luminosity. In M82, NGC 1068, and M83 the line emission peaks strongly at the nuclei. Spatial distributions and velocity profiles of the [C II] line are very similar to the 2.6 mm $J = 1 \rightarrow 0$ emission of CO. The ratio of integrated line intensities of [C II] to CO is constant, for [C II] intensities which vary by a factor of 100 in the extragalactic and galactic sources studied.

The [C II] line is a tracer of molecular clouds and not of atomic hydrogen clouds or tenuous intercloud gas. The 158 μm emission comes from warm ($T \sim 300$ K), dense ($n_H > 10^3$ cm^{-3}) gas at the surfaces of molecular clouds which are exposed to ultraviolet light from embedded OB stars or galactic interstellar radiation fields. The mass of interstellar gas contained in these photodissociation regions can be a significant fraction of the total mass of interstellar gas in galaxies which have large populations of young stars. The variation of [C II] brightness from source to source and its ratio to the integrated infrared continuum intensity agree well with the theoretical prediction that ultraviolet absorption by dust controls the C^+ column density; this limits the hydrogen column density in the C^+ zone to $N_H \lesssim 10^{22}$ cm^{-2} ($A_V \lesssim 5$). The [C II] line is optically thin in most sources, and its brightness is a measure of ultraviolet energy density. The linear proportionality of [C II] to CO intensity suggests that the CO intensity is also affected by ultraviolet energy density and may not reliably measure H_2 mass in galaxies which have large infrared luminosities.

Subject headings: galaxies: nuclei — infrared: spectra — interstellar: abundances — interstellar: matter

I. INTRODUCTION

The far-infrared fine-structure lines of oxygen and carbon are expected to be the major cooling lines for several different components of the interstellar gas in galaxies, including fully ionized gas around early-type stars, partially ionized gas at the interfaces of dense clouds, and tenuous or dense neutral gas. These lines are also a very important diagnostic tool for investigating the physical state of the interstellar medium in galaxies and the heating and cooling mechanisms operating there. The bright [O I], [O III], and [C II] lines have been studied in a number of galactic sources (for reviews see Emery and Kessler 1984; Harwit 1984; Watson 1984). Instrumentation is now sensitive enough to detect these lines in external galaxies; the first observations of the 63 μm [O I] and 88 μm [O III] lines toward the nucleus of M82 were discussed by Watson *et al.* (1984*b*). In this paper we present an investigation of the [C II] 158 μm fine-structure line in six gas-rich galaxies. This is the first detection of this line in extragalactic objects. These data are combined with other measurements of the [C II] line (in various galactic sources) and are compared with studies of the CO $J = 1 \rightarrow 0$ rotational line at 2.6 mm, the H I 21 cm line, and the far-infrared continuum emission in the same objects. Detailed observations of [O I], [O III], and [C II] fine-structure lines toward the nucleus of M82, and an analysis of the state of the interstellar gas in that galaxy, will be discussed in a forthcoming paper (Watson *et al.* 1984*a*).

II. OBSERVATIONS

The data were taken with the 91.4 cm telescope on board the NASA Kuiper Airborne Observatory in three flight series (1983 February and October and 1984 March) from Moffett Field, California, and in one flight series (1983 May) from Richmond Air Force Base, Australia. The spectrometer was the tandem Fabry-Perot described by Storey, Watson, and Townes (1980), with a stressed Ge:Ga photoconductive detector (Haller, Hueschen, and Richards 1979). The system noise-equivalent power (NEP), including all atmospheric and instrumental losses, was 3×10^{-14} W Hz$^{-1/2}$ in 1983 February, 9×10^{-15} W Hz$^{-1/2}$ in 1983 May, and 6–8 $\times 10^{-15}$ W Hz$^{-1/2}$ in 1983 October and 1984 March. The beam size was 60″ (FWHM), with a total solid angle of 9×10^{-8} sr, corresponding to a 70″ equivalent disk. The rest wavelength of the [C II] $^2P_{3/2} \rightarrow {}^2P_{1/2}$ transition is 157.737 $\pm$ 0.002 μm. This value, derived from observed wavelengths of the [C II] line in Orion (assumed LSR velocity +9 km s^{-1}) and W49N (assumed LSR velocity +5 km s^{-1}), was calibrated relative to a D_2O line at 157.495 μm (F. de Lucia, private communication) and an H_2S line at 157.772 μm (Flaud, Camy-Peyret, and Johns 1983). The relative wavelength calibrations were established by recording interference fringes of a He-Ne laser ($\lambda = 0.6328$ μm) reflected from the scanning Fabry-Perot mirrors. Velocities are accurate to $\pm$10 to $\pm$40 km s^{-1}, depending on velocity resolution and signal-to-noise ratio. Chopper throws were typically 4′–7′, with a chopping frequency of 29 Hz. Table 1 is a list of the center positions, observing dates, FWHM velocity resolutions, and continuum flux densities used for absolute calibration (accuracy $\pm$30%) in all six galaxies. The absolute pointing accuracy was about $\pm$20″,

[1] Department of Physics, University of California, Berkeley.
[2] Department of Physics, California Institute of Technology.

and the relative pointing stability during a typical integration (10–30 min) was better than $\pm 10''$.

In the following discussion, the present [C II] observations are compared extensively with CO $J = 1 \rightarrow 0$ ($\lambda = 2.6$ mm) data. Except for M83 and NGC 5128, enough CO comparison data could be found in the literature. CO observations of the latter galaxies were obtained at the Owens Valley Radio Observatory (OVRO), using the No. 2 telescope of the millimeter-wave interferometer (Leighton 1978), a superconducting quasi-particle mixer receiver (Woody, Miller, and Wengler 1984), and a 500 MHz acousto-optical spectrometer (Masson 1982). The beam size for the OVRO CO observations (60″ FWHM) was very similar to that of the KAO [C II] measurements. In order that these CO observations may be directly compared with the existing CO data, they were calibrated on the Kitt Peak scale (Ulich and Haas 1976), according to which $T_A^* = 60$ K for the CO $J = 1 \rightarrow 0$ line in the Orion Kleinmann-Low nebula.

III. RESULTS

Figures 1–3 show the 158 μm [C II] spectra taken at different positions toward the Ir II galaxy M82 (NGC 3034), the Sb/Seyfert 2 galaxy NGC 1068 (M77) and the Sc/SBb galaxy M83 (NGC 5236). For comparison we show the line profiles of the CO $J = 1 \rightarrow 0$ line observed at about the same positions with similar beam size (Young and Scoville 1984 for M82; Scoville, Young, and Lucy 1983 for NGC 1068). Figure 4 gives the radial distributions of the integrated [C II] and CO line fluxes. In that figure we have also included the distributions of H I optical depth in M82 (Weliachew, Fomalont, and Greisen 1984) and M83 (Rogstad, Lockhart, and Wright 1974) derived from interferometric observations of the 21 cm line. Finally, Table 2 gives a list of [C II] line intensities at the nuclei of the six observed galaxies, in addition to derived parameters such as [C II] line luminosities, C^+ column densities, and hydrogen masses in the C^+ regions. These parameters are computed from equations (A1)–(A5) in Appendix A. To derive column densities and masses, we assume that the [C II] line is optically thin, that the upper level is collisionally populated in the high-density, high-temperature limit (i.e., $n_H \gg 10^3$ cm^{-3} and $T \gg 91$ K) and $[C^+]/[H] \approx 3 \times 10^{-4}$. The column densities and masses thus obtained are lower limits. Table 2 also contains comparisons of the [C II] line with the CO $J = 1 \rightarrow 0$ line and far-IR continuum emission. We have listed the same information for a number of different galactic sources to compare with the extragalactic data (references to the literature are contained in the footnotes to Table 2). The main results are given in the following sections.

a) *Brightness of the* [C II] 158 μm *Line*

The [C II] line is relatively bright in all six observed galaxies. At velocity resolutions of 100–200 km s^{-1} the lines are spectrally resolved. They are typically 4–15 times more intense than the 158 μm continuum emission. About 0.5% of the total infrared luminosity—that is, about 0.5% of the bolometric luminosity in the observed galaxies—emerges in the [C II] line. For comparison, Stacey *et al.* (1984) estimate that the total [C II] luminosity of our own Galaxy is $4 \times 10^7\ L_\odot$, which is 0.2% of the total far-IR luminosity. The [C II] line is as intense in M82, the brightest galaxy sampled, as in the central 5 pc of our Galaxy (Genzel *et al.* 1985) or in the extended [C II] halos of M17 and NGC 2024 (Russell *et al.* 1981; Kurtz *et al.* 1983). The [C II] line in M82 is a factor of 3 less intense than at the center of the Orion region and a factor of 4.4 weaker than the brightest galactic [C II] source detected, the southern H II region G333.6−0.2 (Storey *et al.* 1985). The six galaxies studied, however, are gas-rich systems with large populations of young stars, and the high brightness of the [C II] fine-structure line may not be typical of, for example, earlier type spiral galaxies and less active systems.

b) *Spatial Distribution and Kinematics*

In M82, NGC 1968, and M83, the [C II] emission is sharply peaked at the nucleus and falls off rapidly with distance from the center (Figs. 1–4). The radius at which the [C II] intensity has fallen to half-maximum is 0.4 ± 0.1 kpc in M82, 1.2 ± 0.5 kpc in M83 (along the major spiral arms), and $\lesssim 1.5$ kpc in NGC 1068 (Fig. 4). We find significant emission out to a radius of 1.3 kpc in M82, 3 kpc in M83, and 6 kpc in NGC 1068. There is a marginal detection of the line 8.5 kpc south of the nucleus of NGC 1068.

The [C II] intensity may be enhanced in spiral arms. For example, Figure 3 shows that between spiral arms in M83 (40″ southeast of the nucleus) the 158 μm line has significantly less

TABLE 1

SUMMARY OF [C II] OBSERVATIONS IN EXTERNAL GALAXIES

SOURCE	(0, 0) R.A. (1950)	(0, 0) Decl. (1950)	V_{LSR} (sys) (km s^{-1})	FWHM VELOCITY RESOLUTION[a] (km s^{-1})	DATE OBSERVED	LINE FLUX CALIBRATION[b]
NGC 1068 (M77)	02^{h}40^{m}07^s.2	−00°13′30″	+1120	200	1983 Oct	$S_{158}^{\text{Orion-KL}} = 4 \times 10^4$ Jy $S_{158}^{\text{NGC 1068}} = 1.8 \times 10^2$ Jy
IC 342	03 41 58	67 56 27	+30	200	1983 Oct	$S_{158}^{\text{Orion-KL}} = 4 \times 10^4$ Jy
M82 (NGC 3034)	09 51 44	69 55 00	+220	130	1983 Feb	$S_{158}^{\text{Orion-KL}} = 4 \times 10^4$ Jy
				95	1983 Oct	$S_{158}^{\text{M82}} = 1 \times 10^3$ Jy
				100	1984 Mar	
NGC 5128 (Cen A)	13 22 31.8	−42 45 30	+500	100	1983 May	$S_{158}^{\text{G333.6-0.2}} = 1.6 \times 10^4$ Jy
M51 (NGC 5194)	13 27 46.9	47 27 16	+1470	130	1983 Feb	$S_{158}^{\text{Orion-KL}} = 4 \times 10^4$ Jy
				100	1984 Mar	$S_{158}^{\text{M82}} = 1 \times 10^3$ Jy
M51 H II[c]	13 27 56.8	47 28 56		100	1984 Mar	
NGC 5236 (M83)	13 34 12.0	−29 36 40	+490	100	1983 May	$S_{158}^{\text{G333.6-0.2}} = 1.6 \times 10^4$ Jy

[a] The instrumental line profile is a Lorentzian of equivalent width $\pi/2$ times FWHM.

[b] Absolute calibration of line intensities is obtained from line to continuum flux ratios, assuming a total beam solid angle of 9×10^{-8} sr, and 1 Jy $= 10^{-26}$ W m^{-2} Hz^{-1}. The uncertainty in absolute line fluxes is about $\pm 30\%$ (1 σ).

[c] Coordinates +100″, +100″).

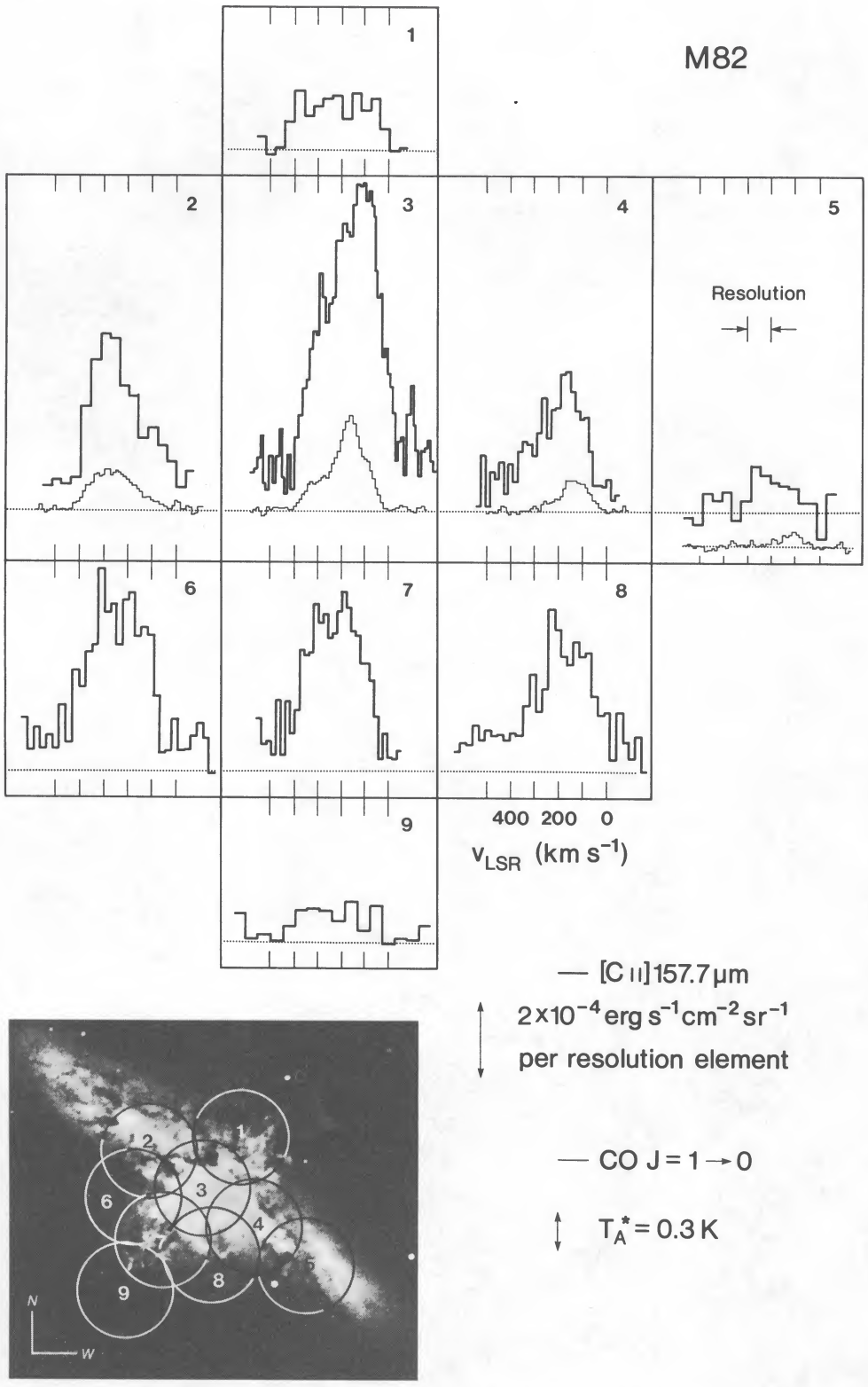

FIG. 1.—Line profiles of [C II] 158 μm emission toward the Ir II galaxy M82. The beam size was 60″ FWHM, and the profiles are ordered along the major axis (*left to right*) and perpendicular to it (*top to bottom*). The individual positions are separated from the center of the galaxy by multiples of ~40″ and are numbered and marked in the adjacent Hα photograph. Positions 1, 2, 4, 5, and 7 were observed in 1983 October, and positions 3, 6, 8, and 9 were observed in 1983 March. The instrumental resolution was 100 km s^{-1}. The dashed horizontal lines indicate zero intensity. Also indicated below the [C II] profiles at positions 2, 3, 4, and 5 are CO $J = 1 \rightarrow 0$ profiles observed at 50″ (FWHM) resolution (from Young and Scoville 1984).

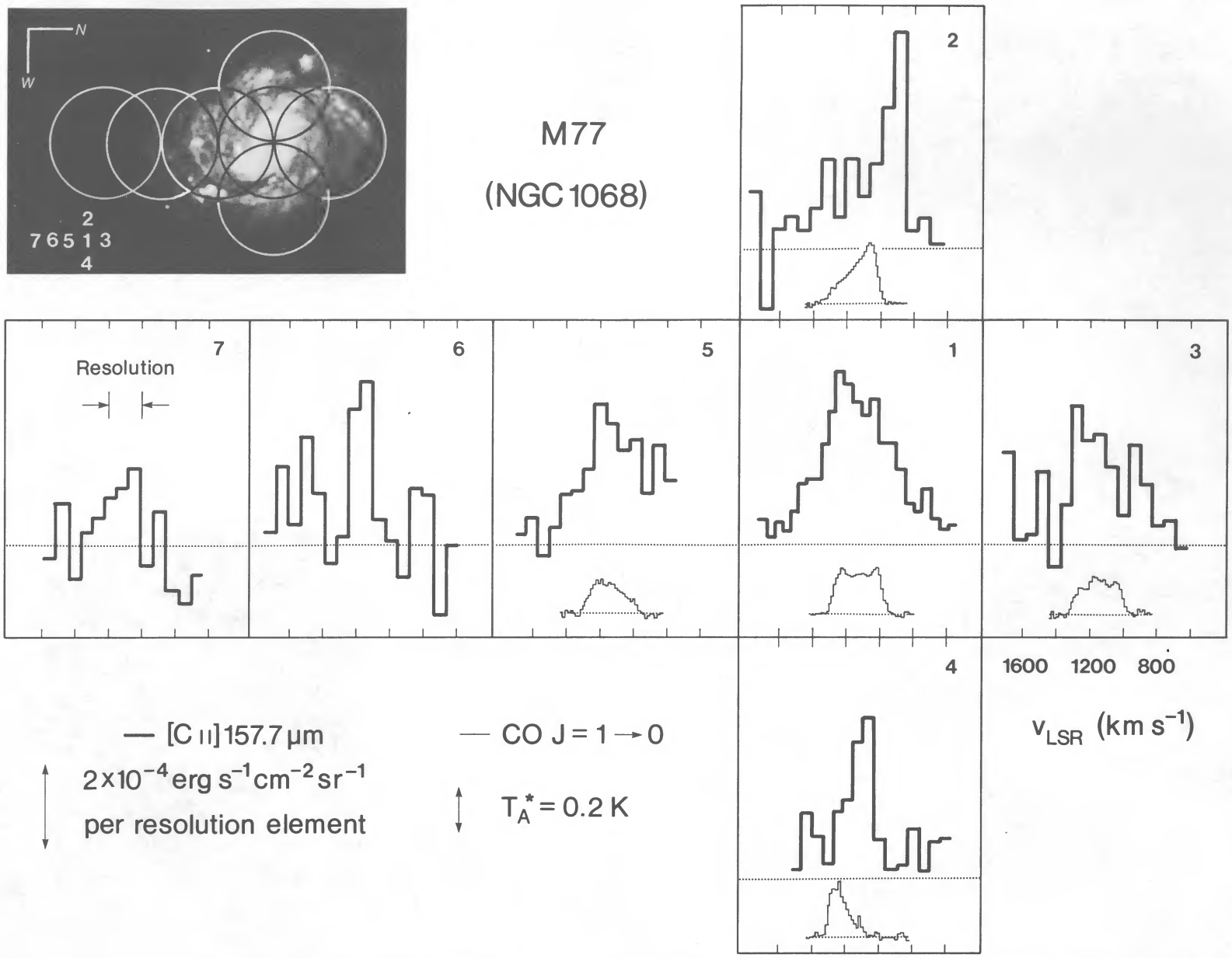

FIG. 2.—[C II] line profiles toward the Sb/Seyfert 2 galaxy NGC 1068, at a velocity resolution of 200 km s^{-1} FWHM and a beam size of 60″ (FWHM). Individual positions are separated by 30″ along the N-S (*right to left*) and E-W (*top to bottom*) directions and are numbered and marked on the adjacent optical photograph. The dashed lines indicate zero intensity. The spectra below the [C II] profiles at the central five postions are CO $J = 1 \rightarrow 0$ profiles from the work of Scoville, Young, and Lucy (1983), taken with a beam size of 50″ (FWHM).

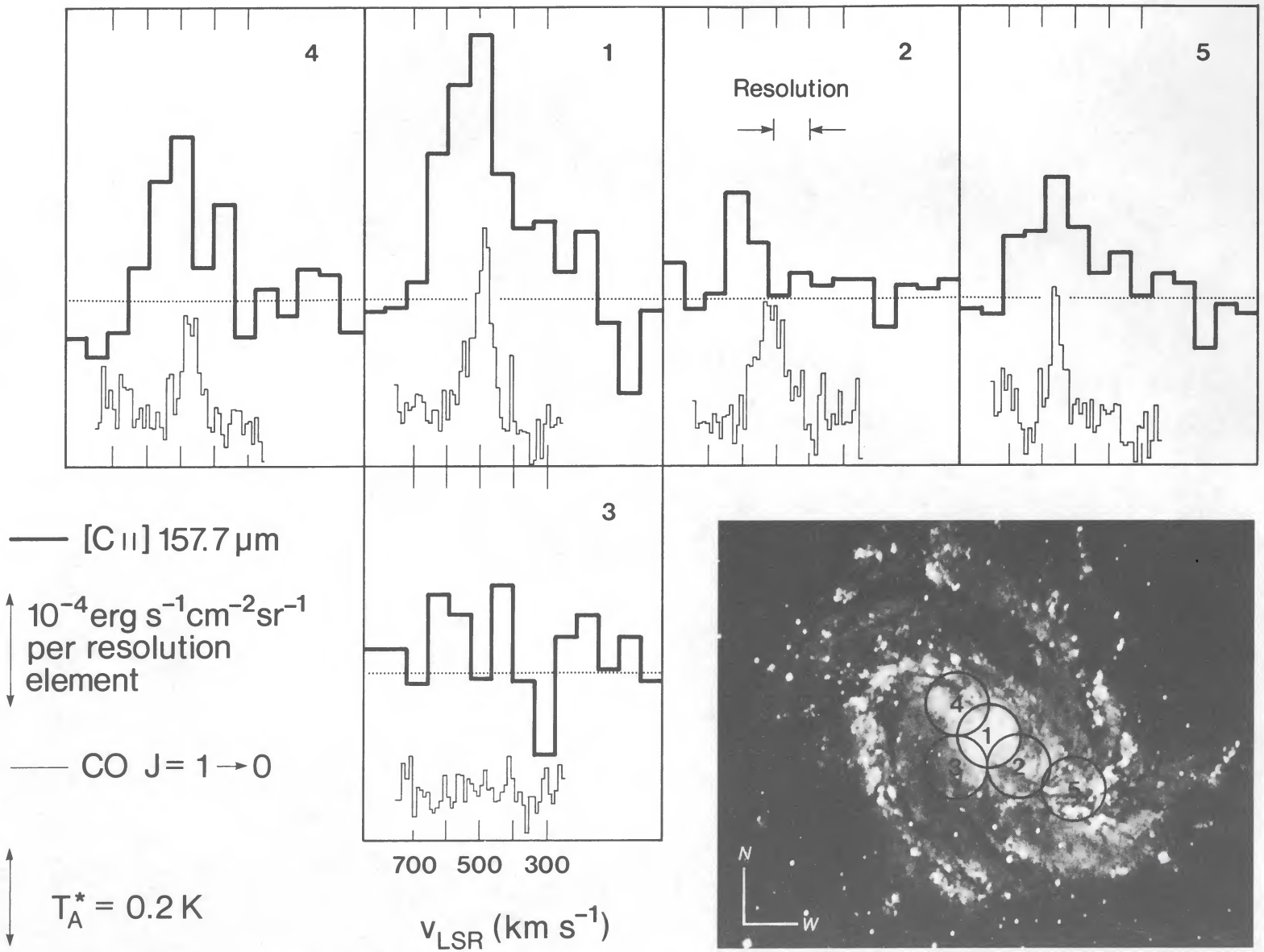

FIG. 3.—[C II] line profiles toward the Sc galaxy M83 (NGC 5236) at a velocity resolution of 100 km s^{-1}. Individual positions are separated by about 40″, are numbered, and are marked on the adjacent optical photograph. Below each [C II] spectrum is a CO $J = 1 \rightarrow 0$ line profile taken with the No. 2 OVRO 10 m telescope (60″ beam size, FWHM).

TABLE 2

PARAMETERS OF [C II] AND CO-EMITTING REGIONS IN GALAXIES AND GALACTIC SOURCES

Object	Distance	Linear Size of Beam (FWHM)	$I_{[C\,II]}$ (ergs s^{-1} cm^{-2} sr^{-1})	$L_{[C\,II]}$ ($L_\odot$)	$N_{C^+}^{MIN\,a}$ (cm^{-2})	$N_H^{MIN}(C^+)^a$ (cm^{-2})	$M(C^+)^{MIN\,a}$ ($M_\odot$)	L_{IR} ($L_\odot$)
External Galaxies								
NGC 1068 (M77)	20 Mpc	5.8 kpc	7.2×10^{-4}	8.0×10^8	4×10^{17}	1.4×10^{21}	4.2×10^8	3×10^{11}
IC 342	3.5	1.0	4.0×10^{-4}	1.4×10^7	2.5×10^{17}	8×10^{20}	7×10^6	4×10^9
M82 (NGC 3034)	3.3	0.96	1.5×10^{-3}	4.6×10^7	9×10^{17}	3×10^{21}	2.4×10^7	3×10^{10}
NGC 5128 (Cen A)	4	1.2	3.0×10^{-4}	1.3×10^7	2×10^{17}	6×10^{20}	7×10^6	...
M51 (NGC 5194)	9.7	2.8	1.7×10^{-4}	4.5×10^7	1×10^{17}	3.5×10^{20}	2.3×10^7	5×10^9
M51 H II (NGC 5194)	...	2.8	7.0×10^{-5}	1.8×10^7	4×10^{16}	1.5×10^{20}	9.5×10^6	2.8×10^9
M83 (NGC 5236)	7.9	2.3	5.0×10^{-4}	8.7×10^7	3×10^{17}	1×10^{21}	4.5×10^7	2×10^{10}
Galactic Sources								
Orion (M42)	0.48 kpc	0.14 pc	5.0×10^{-3}	3.2	3×10^{18}	1×10^{22}	1.7	1×10^5
		0.7	3×10^{-3}	55	1.8×10^{18}	6×10^{21}	30	2×10^5
NGC 2024	0.48	0.7	1.7×10^{-3}	30	1×10^{18}	3.4×10^{21}	15	3×10^4
		3	7×10^{-4}	5.7×10^2	4.2×10^{17}	1.4×10^{21}	1.2×10^2	3×10^4
NGC 2023	0.48	0.14	6.3×10^{-4}	0.41	3.8×10^{17}	1.3×10^{21}	0.21	1×10^5
B 35	0.40	0.12	$< 3 \times 10^{-5}$ (3 σ)	...	...	...	...	...
G333.6−0.2	4	1.2	6.6×10^{-3}	3.0×10^2	4×10^{18}	1.3×10^{22}	1.5×10^2	3×10^6
		4.7	1.3×10^{-3}	8.0×10^2	8×10^{17}	2.6×10^{21}	4.3×10^2	5×10^6
Sgr A	10	2.9	1.5×10^{-3}	4.2×10^2	9×10^{17}	3×10^{21}	2×10^2	5×10^6
$l = 2°$ and 7°	~8	12	1×10^{-3}	7×10^3	6×10^{17}	2×10^{21}	3×10^3	...
M17	2.5	4.0	2×10^{-3}	1×10^3	1.2×10^{18}	4×10^{21}	6×10^2	3×10^6
		10	1×10^{-3}	4×10^3	6×10^{17}	2×10^{21}	2×10^3	5×10^6
W49N	14	4.1	2.8×10^{-3}	1.5×10^3	1.7×10^{18}	6×10^{21}	8×10^2	5×10^6
DR 21	3	0.87	1.7×10^{-3}	43	1.0×10^{18}	3.4×10^{21}	22	1.5×10^5
NGC 7027	1.1	0.32	3.8×10^{-4}	1.3	2.4×10^{17}	8×10^{20}	0.7	9×10^3

TABLE 2—*Continued*

Object	ϵ_{IR} [b] (6×10^{-13} ergs cm^{-3})	I_{CO}^{*} [c] (K km s^{-1})[d]	$N_{CO}^{MIN\,e}$ (cm^{-2})	$N_{H_2}^{MIN}(CO)^e$ (cm^{-2})	$N_{H_2}^{*}(CO)^f$ (cm^{-2})	$I_{[C\,II]}/I_{CO}^{*}$	$M_H^{MIN}(C^+)/M_{H_2}^{MIN}(CO)$	References
External Galaxies								
NGC 1068 (M77)	3×10^2	60	1.5×10^{17}	2×10^{21}	2×10^{22}	7.5×10^3	0.035–0.35	1
IC 342	1×10^2	40	1.0×10^{17}	1.5×10^{21}	1.5×10^{22}	6.3×10^3	0.03–0.3	2
M82 (NGC 3034)	1×10^3	170	4.5×10^{17}	6×10^{21}	7×10^{22}	5.5×10^3	0.03–0.3	3
NGC 5128 (Cen A)	...	...	...	...	...	...	...	
M51 (NGC 5194)	20	30	7.5×10^{16}	9×10^{20}	1×10^{22}	3.5×10^3	0.02–0.2	4
M51 H II (NGC 5194)	10	8	2.0×10^{16}	2.4×10^{20}	2.7×10^{21}	5.5×10^3	0.03–0.3	4
M83 (NGC 5236)	1×10^2	30	7.5×10^{16}	9×10^{20}	1×10^{22}	1.0×10^4	0.05–0.5	5
Galactic Sources								
Orion (M42)	1.5×10^5	360	9.2×10^{17}	1×10^{22}	1.5×10^{23}	8.7×10^3	0.05–0.5	6
	1.0×10^4	200	5×10^{17}	6×10^{21}	7×10^{22}	9.4×10^3	0.05–0.5	7
NGC 2024	1.5×10^3	...	...	...	...	...	...	8
	80	...	...	...	...	...	...	8
NGC 2023	...	90	2.3×10^{17}	3×10^{21}	3.5×10^{22}	4.4×10^3	0.02–0.2	9
B 35	~6	~20	5×10^{16}	6×10^{20}	6×10^{21}	$\leq 9 \times 10^2$	...	10
G333.6−0.2	7×10^4	...	...	...	...	...	...	11
	4×10^3	...	...	...	...	...	...	
Sgr A	2×10^4	160	4.1×10^{17}	5×10^{21}	6×10^{22}	5.9×10^3	0.03–0.3	
$l = 2°$ and 7°	...	150	3.8×10^{17}	5×10^{21}	6×10^{22}	4.2×10^3	0.02–0.2	12
M17	5×10^3	...	...	...	...	...	...	13
	1×10^3	...	...	...	...	...	...	13
W49N	9×10^3	400	1.0×10^{16}	1.5×10^{22}	1.5×10^{23}	4.4×10^3	0.02–0.2	14
DR 21	6×10^3	220	5.6×10^{17}	7×10^{21}	8×10^{22}	4.8×10^3	0.03–0.3	15
NGC 7027	2×10^3	38	9.6×10^{16}	1×10^{21}	1.5×10^{22}	6.2×10^3	0.03–0.4	16

[a] Minimum column densities and masses calculated under the assumptions that [C II] line is optically thin and population is distributed according to statistical weights t high density and temperature (Appendix A), and that $[C^+]/[H] = 3 \times 10^{-4}$.

[b] Calculated from total far-IR luminosity using $\epsilon_{IR} = L_{IR}/(\pi c R^2)$, where c is the speed of light and R is the radius of the region in cm.

[c] Values for T_A^* are on the Kitt Peak scale, for which T_A^*(Orion) = 60 K (Scoville and Young 1983).

[d] 1 K km $s^{-1} = 1.6 \times 10^{-9}$ ergs s^{-1} cm^{-2} sr^{-1}.

[e] Assuming optically thin emission and $T_{kin} = 40$ K; $[CO]/[H_2] = 8 \times 10^{-5}$ (Frerking, Langer, and Wilson 1982).

[f] Using N_{H_2} (cm^{-2}) $= 4 \times 10^{20} I_{CO}^{*}$ (K km s^{-1}) (Young and Scoville 1982; Sanders, Solomon, and Scoville 1984).

REFERENCES.—(1) Telesco *et al.* 1984; Scoville, Young, and Lucy 1983; Rickard *et al.* 1977. (2) Becklin *et al.* 1980; Young and Scoville 1982. (3) Telesco and Harper 1980; Young and Scoville 1984; Olofsson and Rydbeck 1984. (4) Telesco and Harper 1980; Smith 1982; Scoville and Young 1983; Rickard *et al.* 1977. (5) Telesco and Harper 1980; Combes *et al.* 1978; Rickard *et al.* 1977. (6) Ellis and Werner 1984; this paper. (7) Russell *et al.* 1980. (8) Kurtz *et al.* 1983; Russell *et al.* 1980. (9) Jaffe *et al.* 1985; Milman *et al.* 1975; Harvey, Thronson, and Gatley 1980. (10) Jaffe *et al.* 1985; Lada and Black 1976. (11) Storey *et al.* 1985; Hyland *et al.* 1980. (12) Stacey *et al.* 1984; Bania 1977. (13) Russell *et al.* 1981; Harper *et al.* 1976; Gatley *et al.* 1979. (14) This paper; Harvey, Campbell, and Hoffman 1977; Mufson and Liszt 1977. (15) Ellis and Werner 1984; Harvey, Campbell, and Hoffman 1977. (16) Moseley 1980; Telesco and Harper 1977; Ellis and Werner 1984.

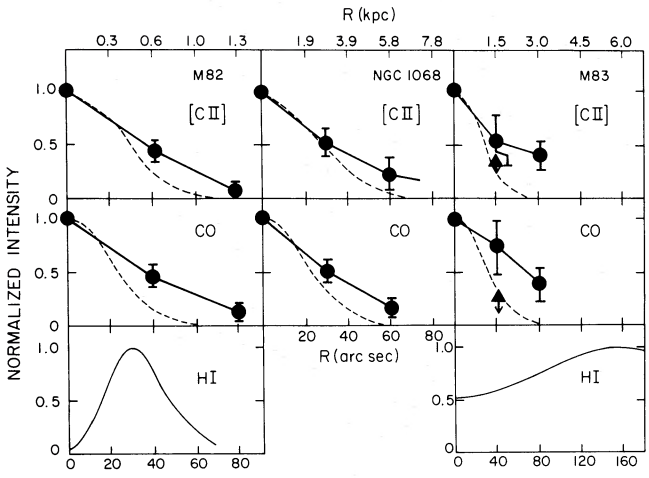

FIG. 4.—Spatial distribution of [C II], CO, and H I gas in M82, NGC 1068, and M83, as a function of distance from the nucleus. The data are normalized to the peak value and are averages of measurements along different position angles. The triangles in the [C II] and CO data of M83 represented measurements 40″ southeast of the nucleus, off the the main spiral arm. The beam profile is also indicated for [C II] and CO (*dashed curves*). The CO data come from the work of Young and Scoville (1984) (M82), Scoville, Young, and Lucy (1983) (NGC 1068), and this paper (M83). The H I values are interferometric measurements of Weliachew, Fomalont, and Greisen (1984) (M82) and Rogstad, Lockhart, and Wright (1974) (NGC 5236).

intensity than at the positions which are located on the main spiral feature (40″ northeast and 40″ southwest of the nucleus).

The [C II] kinematics derived from the line profiles in the central region of NGC 1068 and M83 are consistent with the kinematics deduced from other tracers of interstellar gas such as forbidden lines and the CO $J = 1 \rightarrow 0$ line. The kinematics of [C II] in M82 are also in good agreement with the CO kinematics and will be discussed in detail by Watson *et al.* (1984*a*).

c) Correlation between [C II] *and* CO *Emission*

One of the most striking results of our investigation is the very good correlation of the [C II] fine-structure line emission with CO $J = 1 \rightarrow 0$ emission in terms of large-scale distribution, line profile, and integrated line intensity. Within the measurement uncertainties, the [C II] and CO lines have identical large-scale spatial distributions in M82, NGC 1068, and M83 (Fig. 4). The line profiles at most positions are similar, considering the poorer velocity resolution and pointing accuracy of the [C II] observations. Furthermore, the ratio of [C II] to CO line intensities is *constant* within the three galaxies mapped, as well as in the other galaxies and galactic sources listed in Table 2. Figure 5*a* shows that CO and [C II] line intensities are proportional to each other over *two orders of magnitude* in intensity. The linear correlation in Figure 5*a* is even more remarkable, since it includes galaxies of different type and orientation in addition to galactic sources of widely differing character, ranging from the galactic center to large-scale halos of molecular clouds and a planetary nebula. The only exception to the good correlation is B35, which will be discussed in Jaffe *et al.* 1985 (see also Lada *et al.* 1982). On the average, the 158 μm line is about 4400 times more intense than the $J = 1 \rightarrow 0$ CO line[3] if both are expressed in ergs s^{-1} cm^{-2} sr^{-1}.

[3] Using $I_{CO} = 1.5 I^{*}_{CO}$.

d) Correlation with Far-Infrared Continuum

The [C II] intensity is well correlated with the intensity and distribution of the far-IR continuum. The far-IR continuum emission originates from warm dust and thereby marks the location of early-type stars. Since the C^+ column density is a function of UV energy density, it also will be maximized in regions where there are hot young stars. Thus, as the star formation rate increases, the far-IR continuum and [C II] intensities also increase (see Appendix A; cf. Telesco and Harper 1980; Rieke and Lebofsky 1979; Telesco *et al.* 1984). In contrast to the linear correlation of CO and [C II] intensities, the [C II] brightness does not scale linearly with the energy density of the far-IR radiation field. Figure 5*b* and Table 2 show that the ratio of [C II] line brightness to far-IR continuum energy density for the galaxies is more than one order of magnitude larger than for either Orion or G333.6−0.2, the objects which have the most intense infrared radiation fields. The [C II] brightness is only 3–4 times lower in M82 than in Orion, while the far-IR continuum energy density is two orders of magnitude lower. Hence, either the production efficiency of C^+ ions decreases with increasing UV energy density or the 158 μm line is optically thick in the galactic sources.

e) Correlation with Neutral Atomic Hydrogen

In contrast to the good correlation seen with molecular gas, the large-scale [C II] distributions in M82 and M83 are not similar to the neutral atomic hydrogen distributions. This is shown in Figure 4, where the 21 cm data of Weliachew, Fomalont, and Greisen (1984) for M82 and Rogstad, Lockhart, and Wright (1974) for M83 exhibit H I column density minima at the nuclei and maxima in rings at radii of $\sim$0.5 kpc in M82 and $\sim$5.5 kpc in M83. As emphasized by observers of extragalactic CO emission (see Rickard *et al.* 1977; Young and Scoville 1982; Morris and Rickard 1982), this appears to be a general trend. The H I distribution either is flattened or has a minimum at the nuclei of most observed late-type galaxies, while the CO distribution is peaked there. In addition to the lack of large-scale correlation, the brightness of the [C II] emission from most of the sources listed in Table 2 is several orders of magnitude higher than expected from H I clouds. This will be shown in the next section.

IV. DISCUSSION

In the following, we discuss the origin of [C II] line emission and the characteristics of [C II] regions in gas-rich galaxies. We compare our observations with recent theoretical models and estimate the density and temperature in photodissociation regions located on the edges of molecular clouds. We also discuss the implications of the CO/[C II] correlation for the interpretation of CO data. It should be emphasized that our conclusions probably apply only where UV fields are very intense, such as in star formation regions and galactic nuclei having large populations of young stars. The basic physics of the C^+ $^2P_{3/2} \rightarrow {}^2P_{1/2}$ transition and the dependence of [C II] line intensity on hydrogen number density, column density, and temperature are discussed in Appendix A. In Appendix B we give a more detailed discussion and comparison of [C II] and CO line intensities, optical depths, and cooling.

a) The [C II] *Emission Comes from Molecular Clouds*

The data (Figs. 1–5*a*; Table 2) clearly show that the [C II] line is well correlated in large-scale distribution, flux, and profile with CO $J = 1 \rightarrow 0$ rotational emission. This implies

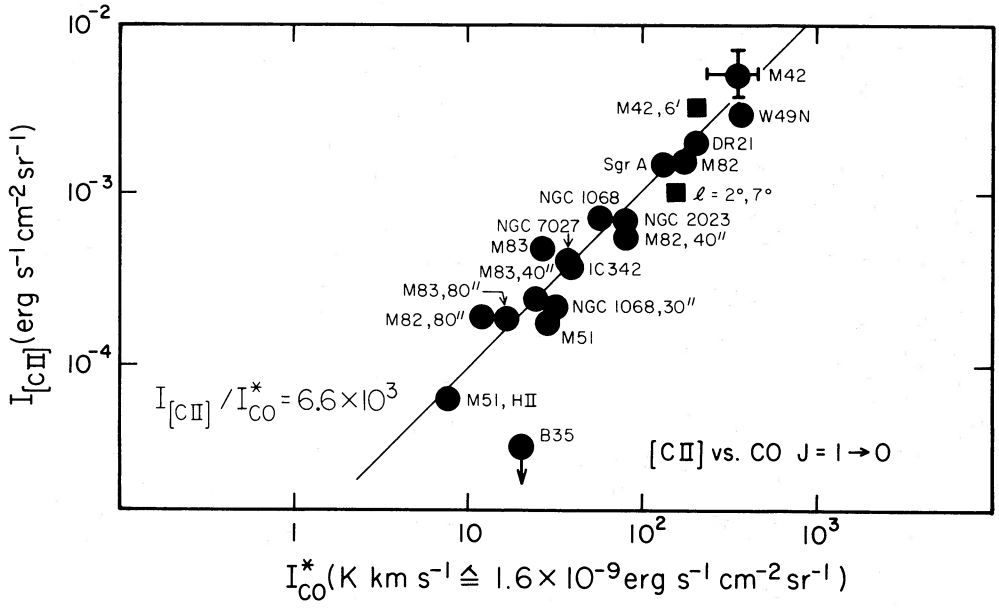

FIG. 5*a*

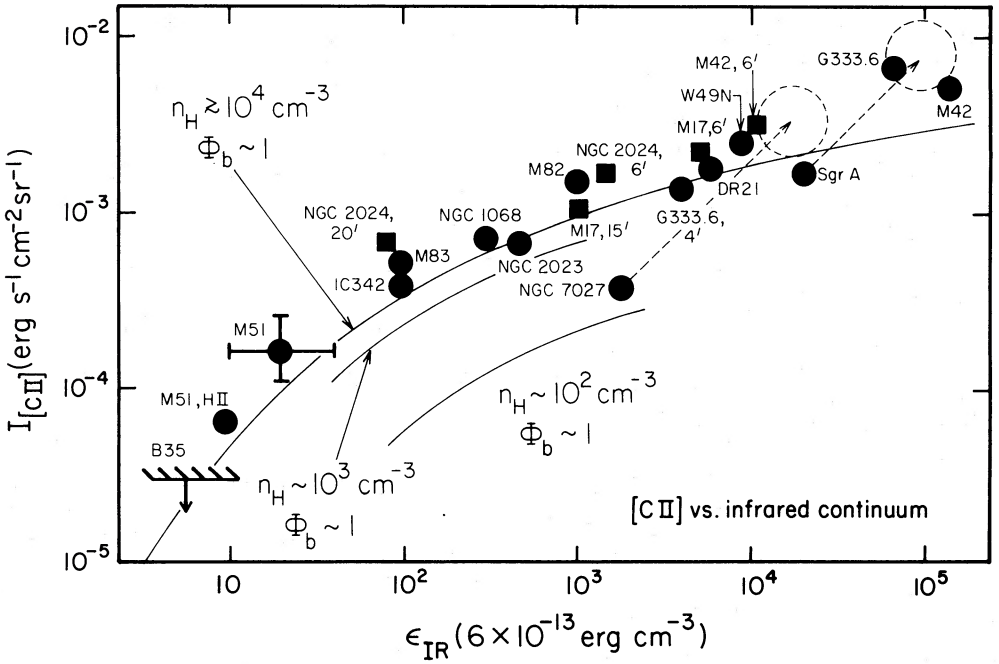

FIG. 5*b*

FIG. 5.—(*a*) Correlation between [C II] and CO integrated line intensities. The CO T_A^* values are on the "Kitt Peak scale" (T_A^* = 60 K for Orion). Data are taken from Table 2. A typical error is shown at the upper right (for Orion). The thin line represents the best fit line. To convert the Kitt Peak T_A^* values to main-beam brightness temperature, multiply by 1.5. This changes the slope of the linear correlation from 6600 to 4400. (*b*) Correlation between [C II] integrated line intensities and ϵ_{IR}, the total infrared energy density, computed from the IR continuum luminosities given in Table 2. A typical error bar is shown at the lower left (for M51). The thin curves represent the predicted [C II] brightness as a function of radiation energy density for hydrogen densities $\gtrsim 10^4$, 10^3, and 10^2 cm^{-3} and unit beam filling factor (from Tielens and Hollenbach 1984). The thin dashed arrow and circle show where Sgr A and NGC 7027 would be located if the line and continuum data were corrected for the low filling factors (see text).

that the C^+ fine-structure line is associated with molecular clouds. A similar conclusion has been reached by Stacey *et al.* (1984) for the large-scale [C II] emission in our Galaxy from a comparison of the scale height of the [C II] and CO distributions at low galactic longitudes. At the surfaces of molecular clouds, where most of the energy from ultraviolet radiation is deposited and C^+ is very abundant, the [C II] 158 μm fine-structure line may be one or two orders of magnitude more important for cooling than the rotational lines of CO (see Appendix B). Furthermore, the total [C II] luminosity may be up to one order of magnitude *smaller* than the line luminosity of the 63 μm transition of [O I] in high-density regions such as Orion, Sgr A, and M82 (Ellis and Werner 1984; Genzel *et al.* 1985; Watson *et al.* 1984*a*). Hence, for molecular clouds which are primarily heated internally by UV light from embedded stars or externally by intense interstellar radiation fields, the far-IR fine-structure lines of C^+ (and O^0) can dominate the total line cooling. C^+ regions are produced by 912–1101 Å radiation present both at the outer parts of molecular clouds, where gas and dust are immersed in the general interstellar UV field, and within clouds wherever OB stars are located. These "photodissociation" or "interface" regions, where molecular photodissociation and photoelectric gas heating by UV radiation are important, have been discussed by Werner (1970), Walmsley (1975), Glassgold and Langer (1975), Langer (1976), Gerola and Glassgold (1978), de Jong (1977), de Jong, Dalgarno, and Boland (1980), and, most recently, by Tielens and Hollenbach (1984, hereafter TH). The latter work predicts far-IR and millimeter-wave intensities as a function of hydrogen density and UV energy density. The most important results of these models are the following:

1. Between the edge of the cloud and its molecular interior, there is a region of hydrogen column density $N_H \lesssim 10^{22}$ cm^{-2} ($A_V < 5$), where the gas (excluding hydrogen) is predominantly atomic (O^0, C^0) or ionic (C^+, Fe^+, Si^+, Mg^+). Due to self-shielding, hydrogen becomes molecular at a significantly smaller depth in the cloud ($A_V \sim 1$–2). Gas in this region is heated predominantly by photoelectric emission from grains (deJong 1977).

2. The most important gas cooling lines are the far-IR fine-structure lines of [O I], [C II] and, to a lesser degree, [C I], [Si II], and [Fe II]. The 158 μm line of C^+ dominates at low densities ($n_H \lesssim 10^3$ cm^{-3}), temperatures ($T < 200$ K), and UV fields, and the 63 μm [O I] line dominates at high densities, temperatures, and UV fields.

3. The depth of the C^+ region (and the column density of C^+) is determined by UV absorption by dust and not by a balance between photoionization of C and recombination of C^+. The C^+ column densities, therefore, only scale approximately logarithmically with the energy density of the UV radiation field.

4. Beyond $A_V > 5$ the gas is mostly molecular, although a large fraction of the oxygen is atomic to $A_V \geq 10$. For $A_V > 5$, most of the gas-phase carbon is in CO. The excitation temperature of the CO $J = 1 \rightarrow 0$ line in this outer region depends strongly on UV energy density.

b) *How Much* [C II] *Emission Comes from Other Components of Interstellar Gas?*

We estimate that components of interstellar gas other than photodissociation regions do not significantly contribute to the observed [C II] brightness, because of insufficient temperature, number density, or column density. Table 3 is a list of [C II] line intensities, expected from diffuse H I gas, H I clouds, compact H II regions and extended low-density H II regions, all computed from parameters estimated for these components in our Galaxy (note that H I clouds may be partially coincident with the atomic hydrogen shells of photodissociation regions; see Mebold *et al.* 1982). We have used the densities, temperatures, and column densities listed in Table 2, and computed $I_{[C\,II]}$ from equations (A1) and (A3) in Appendix A, assuming a face-on galaxy with a maximum scale height (full width) of $z = 1$ kpc. For the intensities listed, we have assumed a beam filling factor of 1.

With the exception of ionized gas in dense, compact H II regions (component 3[i] in Table 3), only warm, dense gas in photodissociation regions of molecular clouds (component 4) can account for the [C II] intensities measured for most sources in Table 2 ($> 10^{-4}$ ergs s^{-1} cm^{-2} sr^{-1}). Compact H II regions, however, are usually embedded in dense molecular clouds, and the [C II] emission of gas within the H II region is much smaller than the [C II] emission from the surrounding photodissociation region (component 4[ii] in Table 3; see Russell *et al.* 1981; Ellis and Werner 1984). Furthermore, on a large scale the filling factors of components 3(i) and 4(ii) can be expected to be smaller than that of 4(i). Finally, [C II] emission from extended, low-density H II regions (Mezger 1978) may account for a small fraction of the total [C II] line emission (see Stacey *et al.* 1984).

TABLE 3

CALCULATED [C II] 158 μm INTENSITIES FROM DIFFERENT COMPONENTS OF INTERSTELLAR GAS

Component	n_H (cm^{-3})	T (K)	N (cm^{-2}) (H I + H_2)	$I_{[C\,II]}$[a]	Volume Filling Factor[b]	Reference
1. Hot, intercloud H I gas	$\gtrsim 10^{-1}$	10^3	$10^{19.5}$	$10^{-6.7}$	$\gtrsim 10\%$	1
2. H I clouds (shells of H_2 clouds)	$\leq 10^1$	10^2	10^{21}	$\leq 10^{-6}$	$\geq 1\%$	1
3. H II regions						
i) Compact H II	$10^{2\pm1}$	10^4	$10^{20.7}$	$10^{-3.6}$	$< 1\%$	
ii) Extended, low-density H II regions	$10^{0.5}$	10^4	10^{21}	$10^{-4.2}$	1%–10%	2
4. Photodissociation regions						
i) Outer edges of molecular clouds						
ii) Internally heated interfaces (embedded OB stars)	10^2–10^3	$10^{2.5}$	$10^{21.5}$	$\geq 10^{-4}$–10^{-3}	$\gtrsim 1\%$	3
	10^4–10^5	$10^{2.5}$	10^{22}	$10^{-2.3}$	$< 1\%$	3

[a] Using eq. (A1), assuming $[C^+]/[H] = 3 \times 10^{-4}$, face-on galaxy (scale length ~ 1 kpc), filling factor = 1.
[b] Expected for galaxies.

REFERENCES.—(1) Mebold *et al.* 1982; (2) Mezger 1978; (3) Tielens and Hollenbach 1984.

c) Optical Depth of the [C II] *Line*

The large body of observational data on the 2.6 mm CO line clearly shows that CO $J = 1 \rightarrow 0$ emission is very optically thick ($\tau_{CO} \geq 10$) in most galactic and probably many extragalactic sources. The good correlation of [C II] and CO intensities suggests, therefore, that the 158 μm line may also have a high optical depth. In the following we show that the optical depth of the 158 μm line is low in most sources and does *not* significantly exceed unity even for the brightest sources in Table 2.

The [C II] optical depth may be calculated if the C^+ column density is known. As shown in Appendix A, the relationship between $N_H(C^+)$, the hydrogen column density in the C^+ region, and the optical depth of the [C II] 158 μm line at high densities ($n_H \gg 10^3$ cm^{-3}) and temperatures ($T \gg 91$ K) is

$$\tau_{[C\,II]} \approx 0.16 N_H[21] \Delta v_5^{-1} \left(\frac{91\ \text{K}}{T}\right). \quad (1)$$

$N_H[21]$ is the hydrogen column density in units of 10^{21} cm^{-2}, Δv_5 is the FWHM of the [C II] line in units of 5 km s^{-1}, and we have assumed that $[C^+]/[H] \approx 3 \times 10^{-4}$. All models of C^+ regions indicate that hydrogen column densities are $\lesssim 10^{22}$ cm^{-2} (Werner 1970; Walmsley 1975; Langer 1976; Gerola and Glassgold 1978; de Jong, Dalgarno, and Boland 1980; Tielens and Hollenbach 1984). Jaffe and Pankonin (1978) have found the width of C^+ recombination lines to be 5 km s^{-1} (FWHM) in Orion. Furthermore, in Orion, Sgr A, and M82, measurements of the line ratios [C II] 158 μm/[O I] 63 μm and [O I] 63 μm/[O I] 146 μm indicate a gas temperature in Orion of ~ 300 K and an average hydrogen density of $\gtrsim 10^4$ cm^{-3} (assuming low optical depth; see Ellis and Werner 1984; Genzel *et al.* 1985; Watson *et al.* 1984*a*). This density is sufficiently high to thermalize the $^2P_{3/2}$ level. The upper bound for the optical depth calculated from equation (1) is then $\tau_{(C\,II)} = 0.5$.

The [C II] line optical depth may also be estimated from the observed line brightness if line width and beam filling factor Φ_b are measured and if the gas and excitation temperatures of the [C II] emission are known (from the [C II]/[O I] line ratios, for example). Although most of the [C II] sources listed in Table 2 are extended with respect to our 60″ beam, the [C II] emission may be clumpy and fill only a fraction of the beam area, particularly in the external galaxies. Assuming $\Phi_b = 1$ and $\Delta v_{[C\,II]} = 5$ km s^{-1}, the [C II] brightness temperature in the Orion region is 200 ± 40 K. This implies an optical depth of 1 ± 0.4 (for $T_{ex}(C^+) = T_{gas} = 300$ K; Ellis and Werner 1984). In the galactic center, the [C II] lines are spectrally resolved and the brightness temperature is 40 ± 15 K, corrected for a beam filling factor of 0.2 ± 0.1 (Genzel *et al.* 1985). The resultant [C II] optical depth is $\sim 0.03^{+0.06}_{-0.02}$ for a gas temperature of 350 K (Genzel *et al.* 1985). In M82 the beam filling factor of the [C II] emission at any given velocity may be estimated from the apparent brightness temperature of the CO $J = 1 \rightarrow 0$ line (assuming that the CO and [C II] emission fill the same area). Correcting for this filling factor, $\Phi_b = 0.05$, Watson *et al.* (1984*a*) derive a peak [C II] brightness temperature of 50^{+30}_{-10} K, and a gas temperature of 200^{+90}_{-70} K. This implies $\tau_{[C\,II]} = 0.1^{+0.4}_{-0.05}$. A low optical depth for the [C II] line in M82 is also obtained by direct comparison with the CO line. This is discussed in Appendix B. It is shown there that the [C II] line always has an optical depth lower than the CO line by approximately the ratio of temperatures in the [C II] and CO regions ($T_{C^+}/T_{CO} \sim 5$). There is evidence that the CO $J = 1 \rightarrow 0$ line has a moderately low optical depth in M82 ($\tau_{CO} \lesssim 1$–3), and hence in M82 $\tau_{[C\,II]} \leq 0.2$–0.6 (eqs. [B5] and [B6] in Appendix B).

Another estimate of the [C II] optical depth can be made by considering the observed average ratio of CO and [C II] line intensities, which is 4400 (from Table 2). This is very close to the cube of the ratio of wavelengths, which means that the (Rayleigh-Jeans) brightness temperatures of the two lines are about equal if the beam filling factors are similar and both lines are optically thick. Since the gas temperatures in the C^+ and CO regions are much greater than $h\nu/k$ for C^+ and CO (91 K and 5 K), the equivalence of brightness temperatures implies that the gas temperatures in these two regions are equal, i.e. $T_{C^+} = 300 \pm 100$ K $= T_{CO}$ (Appendix B, eqs. [B9] and [B10]). Such high CO temperatures are unlikely in all but the brightest sources. We can conclude that the C^+ line, unlike the CO $J = 1 \rightarrow 0$ line, is *optically thin* in most sources.

d) Mass of [C II] *Regions*

Photodissociation regions may contain a significant fraction of the interstellar gas within the central few kpc of the galaxies listed in Table 2. In the second to last column in Table 2 we have listed the ratios of minimum column densities of hydrogen nuclei in the C^+ zones (high density and temperature limit, $[C^+]/[H] \approx 3 \times 10^{-4}$) to the column densities of hydrogen nuclei derived from CO measurements. If the CO is optically thick and the empirical relation between CO intensity and H_2 column density deduced for molecular clouds in our Galaxy is applicable to external galaxies ($N_{H_2} \approx 4 \times 10^{20} I^*_{CO}$ [K km s^{-1}]; Young and Scoville 1982), the mass in C^+ regions is a relatively small percentage of the total gas mass (i.e., $\sim 3\%$ at very high densities and temperatures and $\sim 10\%$ at $n_H = 10^3$ and $T = 300$ K). This empirical relationship is based on three assumptions: the brightness of the CO line is a measure of the filling factor of clouds in the beam (i.e., the clouds are optically thick), the CO line width scales with the mass of an individual cloud according to the virial theorem, and, finally, all clouds have about the same excitation temperature ($T_{ex} \sim 10$ K) and density structure (see Appendix B). If the CO line emission were optically thin, however, or if the optical depth were significantly smaller than the average value of $\tau_{CO} \sim 10$ assumed for the empirical relationship, the mass in C^+ regions could be a significant fraction ($\gtrsim 25\%$) of the total interstellar gas mass in the galaxies studied (assuming $[CO]/[H_2] \sim 8 \times 10^{-5}$ and $T_{kin} \sim 40$ K). This seems to be true for M82. Table 4 is a list of masses of the different components of the interstellar medium in the central 1 kpc of that galaxy (see also Olofsson and Rydbeck 1984 and Watson *et al.* 1984*a*). The mass of 2.9×10^7 $M_\odot$ in C^+ regions listed in Table 4 is greater than the minimum mass given in Table 2 because of a correction for the finite density and temperature in the C^+ region (Watson *et al.* 1984*a*). Since the CO $J = 1 \rightarrow 0$ line in M82 has moderate to low optical depth (see Appendix B), use of the empirical relationship between integrated CO intensity and hydrogen column density deduced for optically thick clouds may not be correct for this galaxy (Knapp *et al.* 1980; Sutton, Masson, and Phillips 1983; Olofsson and Rydbeck 1984). The molecular mass of 6×10^7 $M_\odot$ deduced in the optically thin limit is also consistent with the mass of warm dust ($T_d \geq 20$ K) in that region if the conversion factor relating dust mass to gas mass derived by Hildebrand (1983) is applicable (Jaffe, Becklin, and Hildebrand 1984). The mass in photodissociation regions in M82 is significantly larger than either the H II or the H I mass. It is about 50% of the mass in molecular clouds and 30% of

TABLE 4

MASSES OF COMPONENTS OF INTERSTELLAR GAS IN M82

Component	Mass ($M_\odot$) (within $D = 60'' = 1$ kpc)	Remarks
C^+ (photodissociation regions)	$(2.9^{+2}_{-1}) \times 10^7$	using $n_H = 10^{4\pm1}$ cm^{-3} and $T = 200$ K, $[C^+]/[H] = 3 \times 10^{-4}$ (Watson *et al.* 1984*a*)
H_2	6×10^7	assuming low optical depth for CO, $[CO]/[H_2] = 8 \times 10^{-5}$ (Olofsson and Rydbeck 1984; Sutton, Masson, and Phillips 1983)
	7×10^6	$N_{H_2} = 4 \times 10^{20} I^*_{CO}$ (K km s^{-1}) (Young and Scoville 1984)
Dust	8×10^7	from 400 μm dust emission, $T_{dust} = 45$ K and $M_{gas}/M_{dust} = 10^2$ (Jaffe, Becklin, and Hildebrand 1984)
H I	1.2×10^7	Weliachew, Fomalont, and Greisen 1984
H II	1×10^7	Rieke *et al.* 1980

the total interstellar gas mass ($M_{gas} = 10^8\ M_\odot$) in the central 1 kpc (see Olofsson and Rydbeck 1984).

However, M82 is probably not similar to the other galaxies in Table 2. The high densities deduced from the far-IR lines and the low optical depth of the CO $J = 1 \rightarrow 0$ and $2 \rightarrow 1$ lines suggest that much of the molecular gas in M82 is contained in a large number of small ($R \sim 1$ pc), dense clouds (cf. Knapp *et al.* 1980; Olofsson and Rydbeck 1984; Watson *et al.* 1984*a*). These clouds are very different from the giant clouds ($R \sim 40 \rightarrow 80$ pc) dominating the molecular gas in the disk of our Galaxy. They also have a large ratio of surface area to volume, which increases the fraction of mass contained in photodissociation regions.

In summary, if the empirical conversion from CO intensity to H_2 column density typical of optically thick clouds in our Galaxy is applicable, and if densities in the photodissociation regions are $\sim 10^3$ cm^{-3} and temperatures are ~ 300 K, then the C^+ regions contain up to 10% of the interstellar gas mass in gas-rich galaxies. In galaxies like M82, photodissociation regions may contain an even larger fraction of the total gas mass [$M(C^+)/M(CO) \sim 0.5$] and may play a dominant role in the overall appearance of the interstellar medium.

e) Dependence of [C II] *Brightness on the Energy Density of the UV Radiation Field*

In Figure 5*b* we have plotted $I_{[C\,II]}$ against ϵ_{IR} (ergs cm^{-3}), where ϵ_{IR} is the energy density of the infrared radiation field derived from the total far-IR flux of the source and expressed in units of the energy density of the local galactic interstellar radiation field ($\epsilon_{ISRF} = 6 \times 10^{-13}$ ergs cm^{-3}). The far-IR continuum data were taken from the literature; references appear in the footnotes to Table 2. The sources listed in Figure 5 and Table 2 radiate largely in the far-IR, and the far-IR luminosity is therefore a good measure of the total UV luminosity (so $\epsilon_{IR} \sim \epsilon_{UV}$), since it comes from dust warmed by UV light (cf. Telesco and Harper 1980). The far-IR continuum and C^+ emission should be well correlated through their mutual dependence on UV flux.

In Figure 5*b* we have plotted the predicted [C II] intensity as a function of ϵ_{IR} ($\sim \epsilon_{UV}$), taken from the models of TH for high UV energy densities and from preliminary calculations by Hollenbach and Tielens (private communication) for low UV energy densities. In addition, we assume a beam filling factor of unity for densities of $n_H \sim 10^4$, 10^3, and 10^2 cm^{-3}. In plotting the TH curves we have assumed that in all sources about 10%–15% of the UV and visible luminosity emerges between 912 and 1101 Å, that is, the same fraction as in the local interstellar radiation field. This fraction may be uncertain by up to a factor of 2, but the [C II] intensity changes slowly with ϵ_{IR}, so this uncertainty should not significantly affect the results (see error bars in Fig. 5*b*). Our conclusions do, however, depend strongly on the UV dust absorption coefficients and gas heating efficiencies assumed in the TH models. From Figure 5*b* we conclude the following:

1. $I_{[C\,II]}$ depends qualitatively on ϵ_{UV} in the manner predicted by TH. The model calculations by TH and others (see the beginning of this section) predict the [C II] line brightness to be a slowly varying function of the energy density of the UV radiation field, since absorption by dust in the C^+ region dominates the transport of 912 to 1101 Å radiation. In the TH models, the "saturation" of [C II] brightness at large ϵ_{UV} is not caused by high optical depth of the 158 μm line but is a result of the logarithmic dependence of C^+ column density on ϵ_{UV} and of the relative importance of C^+ and O^0 cooling ([O I] 63 μm emission dominates at high density and high ϵ_{UV}).

2. In all regions except Sgr A and NGC 7027 (see below), beam filling factors and hydrogen densities must be relatively high ($n_H > 10^3$ cm^{-3}). These conclusions are straightforward if the predictions of TH are taken at face value, since all data points are at or above the $n_H \sim 10^4$ cm^{-3}, $\Phi_b = 1$ model of TH. The conclusions also hold if the models are only used as a qualitative guide and if the curves are moved upward to better fit the Orion, Sgr A, and M82 data, where densities and filling factors are known. As mentioned before, the high ratio of [O I] 63 μm to [C II] line intensities (3–10) in these sources gives direct support for high densities in photodissociation regions ($n_H \geq 10^4$ cm^{-3}). If values of 10^3–10^4 cm^{-3} are characteristic of hydrogen densities at the edges of molecular clouds, densities in the interior of molecular clouds may be even higher. When compared with estimated average densities for giant molecular clouds in our Galaxy, i.e., $\langle n_H \rangle \sim 200$ cm^{-3} (cf. Solomon and Sanders 1980; Blitz and Shu 1980), these high densities suggest that molecular clouds are very clumpy throughout.

3. If the calculations of TH apply, the [C II] intensity measures the energy density of the 912–1101 Å UV radiation field. The [C II] line is optically thin ($\tau_{[C\,II]} \lesssim 1$) and is insensitive to density variations (since the line is collisionally saturated at $n_H > 10^3$ cm^{-3}), temperature variations ($T_{gas} \sim 300$ K $\gg h\nu/k = 91$ K), and filling factor once Φ_b is greater than a few tenths. Hence, the [C II] brightness may be "predicted" on the basis of ϵ_{IR} alone, independent of the character of and distance

to (and hence filling factor of) the source. Figure 5*b* shows that external galaxies have the same [C II] brightnesses as nearby galactic objects having equal ϵ_{IR}. Some of these galactic sources were specifically chosen for observation *because* they had ϵ_{IR} similar to the galaxies (Jaffe *et al.* 1985).

4. There are, however, two significant discrepancies between our data and the theoretical predictions. First, the intensities of most sources lie $\sim 50\%$ above TH's models ($n_H \gtrsim 10^4$ cm^{-3}, $[C^+]/[H] = 3 \times 10^{-4}$). This may be accounted for in several ways. If the fraction of total radiation energy density between 912 and 1101 Å has been underestimated (by a factor ≥ 3), the data would move to the right in Figure 5*b* and agree more closely with theory. Alternatively, if the carbon abundances were higher than solar, the gas heating efficiency was greater, or the UV dust absorptivity was lower than assumed in the models, the TH curves would move up proportionally in Figure 5*b*. Furthermore, an *edge-on* or *limb-brightened* geometry would also make the [C II] line brighter than expected in the plane-parallel model used by TH. Finally, if the total velocity width of the line is substantially larger than the velocity width of a single cloud, the beam filling factor per cloud may be small ($\Phi_{bc} < 1$), but the total beam filling factor of clouds, irrespective of velocity, may exceed unity ($\Phi_b > 1$), producing enhanced integrated line intensities.

5. The second discrepancy is that the [C II] line brightness in Sgr A and NGC 7027 are both less than in other sources having similar ϵ_{IR} and less than predicted by the models. This is most likely due to the low beam filling factors in these sources ($\Phi_b \approx 0.1$–0.3 in Sgr A [Genzel *et al.* 1985] and $\Phi_b = 0.1$ in NGC 7027 for a source size of 20″ [Moseley 1980]), although in NGC 7027 the extremely high effective temperature of the UV radiation field could also play a role. The dashed arrows and circles in Figure 5*b* denote where the sources would be if continuum and line fluxes were corrected for the low filling factor. Note that motion along a 45° line to the lower left and below the TH curves would be typical of any source where the C^+ regions are exposed to a higher UV energy density than estimated from the total observed continuum flux. Such a situation would arise, for example, if the UV sources and [C II] regions were located in small clouds with $\Phi_b < 1$ rather than distributed homogeneously over the beam.

f) *Consequences for the Interpretation of* CO *Lines*

The observations imply that higher [C II] intensity in one source compared with another is a result of larger C^+ column density because of higher UV radiation field density. Higher [C II] intensity, however, does not imply a larger column density of H_2 in molecular clouds. There may be an indirect dependence of [C II] intensity on mass, since the UV energy density scales with the rate of star formation, which may depend on the available gas mass. The dependence of [C II] brightness on the UV field may have a significant impact on the standard interpretation of the CO $J = 1 \rightarrow 0$ line as a direct measure of total hydrogen mass in galaxies. If CO and C^+ regions are intimately connected, as suggested by our data, the stronger UV radiation fields at the nuclei will not only increase the C^+ column density but will also significantly elevate the gas and excitation temperatures of the CO in the molecular layer adjoining the C^+ zone. Since the standard conversion of CO integrated intensity to hydrogen column density, $N_{H_2} = 4 \times 10^{20} I^*_{CO}$, is derived for optically thick galactic clouds where $T \approx 10$ K and density is ~ 200 cm^{-3}, an increase in the CO excitation temperature above 10 K will result in an overestimate of the H_2 mass. In fact, *if* the correlation of [C II] and CO intensities is interpreted as evidence for a constant [C II]/CO intensity ratio per unit surface area of molecular clouds as well as equal filling factors for the two species, then the derived *total* H_2 column density should be approximately the same in all sources studied. This is a consequence of the near unit filling factors and high number densities (above the critical density, the [C II] intensity is roughly independent of density) implied by the [C II] data and the models. If the CO emission is optically thick and has filling factors equal to those of [C II], the source-to-source variation in I_{CO} may be significantly influenced by temperature. This conclusion probably does not apply to molecular clouds in disks of normal spiral galaxies where $\epsilon_{UV} \sim 1$–10 (in units of 6×10^{-13} ergs cm^{-3}), which may not be sufficient to significantly affect the gas temperature in the CO–emitting regions. Furthermore, if the UV radiation responsible for generating C^+ regions is produced primarily by stars embedded *within* molecular clouds, there may be clouds which do not have stars in their interiors and thus produce less [C II] emission than would be expected on the basis of their CO emission alone. Such sources might not fall on the line in Figure 5*a*.

There is other evidence supporting an excitation effect in the CO data, but there are also some problems with this interpretation. Three observations favor the hypothesis that the strong increase in CO $J = 1 \rightarrow 0$ brightness toward the nuclei of gas-rich galaxies is partly an excitation effect and not solely a result of a concentration of molecular mass. First, the dust temperature deduced from far-IR continuum emission decreases from about 50 K in M82 to about 30 K in M51. Dust temperatures in NGC 1068, IC 342, and M83 lie within this range (Telesco and Harper 1980; Becklin *et al.* 1980; Rickard and Harvey 1984). Second, Rickard and Harvey (1983) have reported an increase of dust temperature in the central 1′ of Maffei 2 (see, however, Sargent *et al.* 1984). Finally, molecular clouds close to the center of our Galaxy appear to be significantly warmer than typical clouds in the galactic disk (Liszt and Burton 1978; Güsten, Walmsley, and Pauls 1981; Morris *et al.* 1983), although gas heating mechanisms other than UV heating may be important there. Since far-IR dust temperatures refer to an average through the cloud, variations in the excitation temperature of optically thick CO close to the UV-illuminated cloud edges may be much more pronounced than variations in dust temperature. A dependence of CO excitation temperature on the energy density of the UV radiation field may in part explain the good correlation of the integrated CO intensity with blue light found by Young and Scoville (1982) and Scoville and Young (1983).

There are, however, two problems in attributing the variations in CO brightness to excitation. If the CO emission in M82 were very optically thin, i.e., $\tau \ll 1$, then its very high brightness could not be attributed to high temperature, since, as can be seen from equation (B2), the brightness of optically thin CO is *inversely* proportional to temperature. Furthermore, although there is an apparent correlation of CO/[C II] brightness with dust temperature for the brightest galaxies observed by Scoville and Young (see references), Rickard and Harvey (1984), investigating a larger sample (including all extragalactic CO and far-IR measurements to date), do not find a significant correlation between CO intensity and dust temperature. Finally, we also point out that changes in metallicity may account for some of the [C II] and CO intensity variations.

V. CONCLUSIONS

We have presented observations of the 158 μm fine-structure line of C^+ toward the nuclei of six gas-rich galaxies. These measurements have been compared with observations of CO $J = 1 \rightarrow 0$ and H I 21 cm lines, observations of far-IR continuum emission, and observations of [C II] emission within our Galaxy. The [C II] line comes from dense ($n_H > 10^3$ cm^{-3}), warm ($T \sim 300$ K) gas in UV-illuminated photodissociation regions at the surfaces of molecular clouds. The 158 μm fine-structure line is one of the most important cooling lines in these interface regions, and accounts for about 0.5% of the total far-IR luminosity of galaxies. The [C II] line is probably a prominent cooling line in tenuous H I gas (Jura 1978; Dalgarno and McCray 1972) and in extended H II regions, but the lower densities and column densities in these regions result in a [C II] intensity much lower than that in dense molecular clouds.

The [C II] line intensity is linearly proportional to CO $J = 1 \rightarrow 0$ line intensity, and line profiles and large-scale spatial distributions of the two emission lines are about the same. The spatial distribution of the [C II] emission is also similar to the distribution of far-IR continuum emission from warm dust, but differs from the distribution of neutral atomic hydrogen.

The [C II] line is probably optically thin in all but the brightest galactic sources. Our data are in good agreement with the theoretical prediction that UV absorption by dust, rather than a balance between photoionization and electron recombination, determines the C^+ column density. A detailed comparison of the theoretical models with the data suggests that the observed [C II] brightness is a direct measure of the UV radiation density and is not very sensitive to total gas mass, beam filling factor, temperature, and density toward the nuclei of galaxies with large infrared luminosities.

The brightness of the [C II] line is sharply peaked at the nuclei of the three galaxies we have mapped. This is probably a result of the intense UV fields there, but may also reflect a greater number of molecular cloud complexes in the nuclei. We propose that the strong increase of CO emission toward the nuclei of these and other gas-rich galaxies is not due solely to a large concentration of molecular mass, but may in part be an excitation effect.

The [C II] line is a tracer of molecular clouds, especially those near intense sources of UV radiation. It is interesting to note that the sensitivity of far-IR spectroscopy (for [C II] 158 μm) is *currently* competitive with millimeter-wave observations (of CO $J = 1 \rightarrow 0$) for detecting molecular clouds in external galaxies. If cryogenic telescopes in space become available, far-IR spectroscopy will be superior to millimeter-wave techniques for locating molecular matter.

This research was the result of a number of observing flights on the Kuiper Airborne Observatory, and we thank the staff for their continuing commitment and support. A. Meyer has done an excellent job in tracking. D. M. W. thanks his colleagues at the Owens Valley Radio Observatory, especially C. Masson, for their help with the CO observations of M83 and Cen A. We thank J. Storey and J. Lugten for help with instrument preparation and observations. E. Haller from the UC Berkeley Material Sciences Department has kindly provided us with the Ge:Ga detectors used for the observations. We are also grateful to D. Hollenbach, P. Harvey, L. J. Rickard, A. Tielens, and M. Walmsley for helpful discussions and to H. B. Ellis, D. A. Harper, D. Jaffe, J. Storey, and M. Werner for permission to use data prior to publication. Single-dish observing at OVRO is supported by NSF grant AST-82 14693. Observations on the KAO were supported by NASA grant NAG-253.

APPENDIX A

THE $^2P_{3/2}$–$^2P_{1/2}$ FINE-STRUCTURE LINE OF C^+

The spin-orbit interaction removes the degeneracy of the $J = 3/2$ and 1/2 levels of the ^2P ground term of C^+, yielding a magnetic dipole transition at 157.737 $\pm$ 0.002 μm. The next higher electronic states (^4P, ^2D, and ^2S) are between 6.2×10^4 and 1.4×10^5 K above the ground state and in most astrophysical environments are not significantly populated. The ionization potential of neutral carbon is 11.3 eV (1101 Å); hence all far-UV photons shortward of 1101 Å but longward of the hydrogen continuum edge (912 Å) contribute to the ionization of carbon. As stated by several authors (e.g., Werner 1970; Walmsley 1975; Russell *et al.* 1980, 1981; Stacey *et al.* 1984), most of the C^+ column density is in partially ionized (hydrogen not significantly ionized) "photodissociation" regions which are penetrated by far-UV photons capable of ionizing carbon. These regions may be found in tenuous interstellar gas, in atomic hydrogen clouds at the outer edges of molecular clouds, and, finally, at the interfaces between compact H II regions and the dense clouds in which they are embedded. Carbon is also ionized within H II regions; however, in most cases the C^+ column densities there are significantly smaller than in the partially ionized medium outside H II regions (see Russell *et al.* 1980, 1981).

The [C II] 158 μm fine-structure line emission is excited by collisions with electrons or hydrogen atoms and molecules. Radiative excitation would have to proceed via excitation to the ^2D and ^2S levels by absorption of 1000–1300 Å photons, followed by cascading to $^2P_{3/2}$. In the extragalatic and galactic sources discussed here, however, there are far too few photons in this wavelength range to account for the observed number of 158 μm photons. This situation holds for essentially all forbidden lines of ions and atoms (see, for example, Osterbrock 1974).

For collisional excitation, the integrated line intensity (ergs cm^{-2} s^{-1} sr^{-1}) in the optically thin limit (see also the discussions by Russell *et al.* 1980, 1981; Watson 1984) is given by

$$I_{[\mathrm{C\,II}]} = \frac{h\nu A}{4\pi}\left[\frac{g_u/g_l\, e^{-h\nu/kT}}{1 + g_u/g_l\, e^{-h\nu/kT} + n_{\mathrm{crit}}/n}\right]\chi(\mathrm{C}^+)N_{\mathrm{H}}(\mathrm{C}^+)\Phi_b\,. \tag{A1}$$

The transition energy of the 157.737 μm transition is $h\nu = 1.26 \times 10^{-14}$ ergs, $A = 2.36 \times 10^{-6}$ s^{-1}, the ratio of statistical weights in the upper and lower levels is $g_u/g_l = 2$, $\chi(C^+)$ is the abundance of C^+ relative to hydrogen, $N_H(C^+)$ (cm^{-2}) is the column density of

hydrogen nuclei in the C^+ region and n (cm^{-3}) is the number of density of the collision partner. The beam area filling factor, Φ_b, gives the fraction of the beam filled by C^+ gas. The critical density, n_{crit}, is the number density of collision partners (electrons or hydrogen) at which the collision rate from the upper to the lower level is equal to the spontaneous radiation rate. The term in brackets is equal to the fraction of C^+ ions in the $^2P_{3/2}$ level, n_u/n_{C^+}. For excitation by electrons, $n_{crit} \approx 0.79\ [T\ (K)]^{1/2}$ (Launay and Roueff 1977), where T is the gas temperature. For excitation by atomic hydrogen, $n_{crit} = 3000\ cm^{-3}$, and for molecular hydrogen, $n_{crit} = 5000\ cm^{-3}$, both critical densities being approximately independent of temperature between 60 and 1000 K (Launay and Roueff 1977; Flower and Launay 1977). Outside H II regions, where the electron abundance is $n_e/n_H \sim 3 \times 10^{-4} < n_{crit}(H)/n_{crit}(e) \approx 3 \times 10^{-3}$, collisional excitation is dominated by hydrogen impact. In what follows we will use $n_{crit} = [n_{crit}(H) + n_{crit}(H_2)]/2 \approx 4 \times 10^3\ cm^{-3}$.

At high densities ($n_H \gg 4 \times 10^3$) and temperatures ($T \gg 91$ K), the intensity of the 158 μm line is proportional to the column density of C^+ ions:

$$I_{[C\ II]} = 5 \times 10^{-4} N_{C^+}[17.5]\Phi_b\ \text{ergs s}^{-1}\ \text{cm}^{-2}\ \text{sr}^{-1}\ , \tag{A2}$$

where $N_{C^+}[17.5]$ is the column density of C^+ in units of $3 \times 10^{17}\ cm^{-2}$. In the low-density limit ($n_H \ll 4 \times 10^3\ cm^{-3}$),

$$\begin{aligned} I_{[C\ II]} &= 3.9 \times 10^{-7} e^{-91\ K/T} n_H N_{C^+}[17.5]\Phi_b \\ &= 3.9 \times 10^{-7} e^{-91\ K/T} n_H \chi_{-3.5}(C^+) N_H[21]\Phi_b\ \text{ergs s}^{-1}\ \text{cm}^{-2}\ \text{sr}^{-1}\ , \end{aligned} \tag{A3}$$

where the hydrogen density n_H is in units of cm^{-3}, $\chi_{-3.5}(C^+)$ is the abundance of C^+ in units of 3×10^{-4} (all C is in C^+), and $N_H[21]$ is the column density of H in units of $10^{21}\ cm^{-2}$. The C^+ column densities and associated hydrogen masses listed in Table 2 are lower limits which apply to the case of high density, temperature, and C^+ abundance [$\chi_{-3.5}(C^+) \sim 1$ in eq. (A2)]. The optical depth of the [C II] line is given by

$$\begin{aligned} \tau_{[C\ II]} &= \frac{c^3 A}{8\pi \nu^3 \Delta v}\left[\left(1 + \frac{n_{crit}}{n}\right)e^{h\nu/kT} - 1\right]\left(\frac{g_u/g_l\, e^{-h\nu/kT}}{1 + g_u/g_l\, e^{-h\nu/kT} + n_{crit}/n}\right)N_{C^+} \\ &= 0.24\left[\left(1 + \frac{n_{crit}}{n}\right)e^{91\ K/T} - 1\right]\left(\frac{n_u}{n_{C^+}}\right)N_{C^+}[17.5]\Delta v_5^{-1}\ . \end{aligned} \tag{A4}$$

Δv_5 is the equivalent velocity width of the line in units of 5 km s^{-1}. In the high-density and high-temperature limit, this becomes

$$\begin{aligned} \tau_{[C\ II]} &= 1.63 \times 10^{-1} N_{C^+}[17.5]\Delta v_5^{-1}\left(\frac{91\ K}{T}\right) \\ &= 1.63 \times 10^{-1} \chi_{-3.5}(C^+) N_H[21]\Delta v_5^{-1}\left(\frac{91\ K}{T}\right). \end{aligned} \tag{A5}$$

APPENDIX B

COMPARISON OF [C II] AND CO LINES

In this appendix we give a more detailed analysis of [C II] and CO line intensities, and we discuss the ratio of [C II] and CO optical depths.

I. EXCITATION

Although the Einstein A-coefficient of the [C II] 158 μm line ($2.36 \times 10^{-6}\ s^{-1}$) is 35 times larger than that of the CO $J = 1 \rightarrow 0$ transition ($7.5 \times 10^{-8}\ s^{-1}$), the critical densities of the two transitions, that is, the density at which the A-coefficient equals the downward collision coefficient γ_{ul} ($cm^3\ s^{-1}$), are approximately the same since the collision rates are faster for the C^+ ion [$n_{crit}(C^+) \sim 4 \times 10^3\ cm^{-3}$ and $n_{crit}(CO) \sim 2 \times 10^3\ cm^{-3}$ for collisions with hydrogen]. Hence, the ratio of [C II] to CO line intensities will not be sensitive to density if $n_H \gg 4 \times 10^3\ cm^{-3}$ and densities are approximately the same in the C^+ and CO regions. Gas temperatures, however, may be very different in the two regions. The gas temperature in the C^+ zone has been estimated from far-IR line ratios to be between 200 and 400 K for Orion, Sgr A, and M82, in good agreement with the TH models (Ellis and Werner 1984; Genzel *et al.* 1985; Watson *et al.* 1984*a*). Average gas temperatures in the CO–emitting regions of giant molecular clouds in the disk of our Galaxy are 10–20 K (Solomon and Sanders 1980; Blitz and Shu 1980) but can increase to 30–100 K in cores of molecular clouds (cf. Evans 1981), in the galactic center (Liszt and Burton 1978; Morris *et al.* 1983), or in the UV-illuminated region of Orion-Trapezium (Schloerb and Loren 1982).

II. RATIO OF [C II] TO CO LINES: BOTH LINES OPTICALLY THIN

In the following, we assume that hydrogen densities and gas temperatures are high enough to populate the $J = 1$ level of CO and the $J = 3/2$, 1/2 levels of C^+ according to their statistical weights: $n_H \gg n_{crit}(CO, C^+) \sim (2\text{–}4) \times 10^3\ cm^{-3}$, $T_{CO} \gg 5$ K, $T_{C^+} \gg 91$ K. In this limit, the integrated line intensities (ergs $s^{-1}\ cm^{-2}\ sr^{-1}$) are given in the optically thin approximation as

$$I_{[C\ II]} = 5.2 \times 10^{-4} N_{C^+}[17.5]\left(\Phi_{bc}\frac{\Delta v_{tot}}{\Delta v_c}\right)_{C^+} \tag{B1}$$

and

$$I_{\rm CO} = 1.1 \times 10^{-5} \frac{N_{\rm CO}[17.5]}{T_{\rm CO}\ ({\rm K})} \left(\Phi_{bc} \frac{\Delta v_{\rm tot}}{\Delta v_c}\right)_{\rm CO} . \tag{B2}$$

The expression for [C II] is derived in Appendix A. $N_{\rm C^+}[17.5]$ and $N_{\rm CO}[17.5]$ are the total C^+ and CO column densities in units of 3×10^{17} cm^{-2}. Note that the integrated CO intensities given in Table 2 have to be corrected for beam efficiency ($I_{\rm CO} \approx 1.5 I^*_{\rm CO}$). Φ_{bc} is the beam filling factor at a given velcoity, which is identical with the beam filling factor of *one* cloud if there is only one cloud at each velocity. Δv_c is the velocity width of one cloud and $\Delta v_{\rm tot}$ the total width of the line, summed over all clouds in the beam. Note that $\Delta v_{\rm tot}/\Delta v_c$ is the number of clouds contained in the line profile. Hence, the cloud beam filling factor, irrespective of velocity, is $\Phi_b = \Phi_{bc} \Delta v_{\rm tot}/\Delta v_c$. If the filling factors of C^+ and CO regions are approximately the same (as has been proposed in this paper for nuclei of bright galaxies), the ratio of integrated line intensities is

$$\frac{I_{\rm [C\ II]}}{I_{\rm CO}} = 46 T_{\rm CO}\ ({\rm K}) \left(\frac{N_{\rm C^+}}{N_{\rm CO}}\right) . \tag{B3}$$

The dependence on $T_{\rm CO}$ comes from the CO partition function. With $T_{\rm CO} \sim$ 10–50 K and an observed average intensity ratio of 4.4×10^3, obtained by correcting for main-beam efficiency the value of 6.6×10^3 given in Table 2, we find

$$\left(\frac{N_{\rm C^+}}{N_{\rm CO}}\right) \geq 2\text{–}10 \tag{B4}$$

or

$$\left[\frac{N_{\rm H}({\rm C^+})}{2N_{\rm H_2}({\rm CO})}\right] \geq 0.3\text{–}1 .$$

These values are lower limits calculated using $T_{\rm C^+} \gg 91$ K, rather than $T_{\rm C^+} \sim$ 200–400 K, in equation (A1). For computing the hydrogen column densities, we adopted $[{\rm C^+}]/[{\rm H}] = 3 \times 10^{-4}$ and $[{\rm CO}]/[{\rm H_2}] = 8 \times 10^{-5}$ (Frerking, Langer, and Wilson 1982). Equation (B3) (optically thin limit) implies that photodissociation regions contain a significant fraction of the interstellar gas mass.

III. RATIO OF OPTICAL DEPTHS

In general, the CO $J = 1 \rightarrow 0$ line is more optically thick than the [C II] line. In the high-density and high-temperature limit the [C II] and CO optical depths are given by

$$\tau_{\rm [C\ II]} = 1.46 \times 10^1 \frac{N_{\rm C^+}[17.5]}{T_{\rm C^+}\ ({\rm K})} \Delta v_5^{-1} \tag{B5}$$

and

$$\tau_{\rm CO} = 1.43 \times 10^3 \frac{N_{\rm CO}[17.5]}{T^2_{\rm CO}\ ({\rm K})} \Delta v_5^{-1} , \tag{B6}$$

where Δv_5 is the equivalent line width in units of 5 km s^{-1}. If the column densities are expressed in terms of the (optically thin) line intensities, the ratio of optical depths is

$$\frac{\tau_{\rm [C\ II]}}{\tau_{\rm CO}} = 2.2 \times 10^{-4} \left(\frac{T_{\rm CO}}{T_{\rm C^+}}\right)\left(\frac{I_{\rm [C\ II]}}{I_{\rm CO}}\right) . \tag{B7}$$

With $I_{\rm [C\ II]}/I_{\rm CO} = 4.4 \times 10^3$,

$$\left(\frac{\tau_{\rm [C\ II]}}{\tau_{\rm CO}}\right) \approx \left(\frac{T_{\rm CO}}{T_{\rm C^+}}\right) . \tag{B8}$$

The optical depth of the [C II] line, therefore, is considerably smaller than that of the CO line, since the gas temperature in the C^+ region is about 5 times larger than in the CO region. For example, the ratios of ^{12}CO $J = 2 \rightarrow 1$ to $1 \rightarrow 0$ lines and the ^{12}CO to ^{13}CO $J = 1 \rightarrow 0$ lines may be interpreted as evidence for moderate to low optical depth of the ^{12}CO $J = 1 \rightarrow 0$ line in the central 1 kpc of M82 ($\tau_{\rm CO} \lesssim$ 1–3; Knapp *et al.* 1980; Stark 1982; Sutton, Masson, and Phillips 1983; Olofsson and Rydbeck 1984; Stark and Carlson 1984). Hence, $\tau_{\rm [C\ II]}({\rm M82}) \lesssim 0.2\text{–}0.6$. This assumes that the CO clouds are not hotter on the outside than the inside, which would make $T_{^{12}{\rm CO}}(2 \rightarrow 1) > T_{^{12}{\rm CO}}(1 \rightarrow 0) > T_{^{13}{\rm CO}}(1 \rightarrow 0)$. The observed ratios could then result from optically thick gas (Young and Scoville 1984).

IV. RATIO OF [C II] TO CO LINES: CO OPTICALLY THICK

If the CO line is optically thick, its integrated intensity in ergs s^{-1} cm^{-2} sr^{-1} is given by

$$I_{\rm CO}(\tau_{\rm CO} > 1) = 1.6 \times 10^{-9} T_{\rm CO}\ ({\rm K})\ \Delta v_c\ ({\rm cm\ s^{-1}})\ N_c \Phi_{bc} , \tag{B9}$$

where $N_c = \Delta v_{\rm tot}/\Delta v_c$ is the number of clouds of velocity width Δv_c contained in the line profile. The line intensity may still be sensitive to column density if $\Phi_{bc} < 1$ (note, however, that $\Phi_b = N_c \Phi_{bc}$ may exceed 1) and if all clouds have similar characteristics

(T_{CO}, ratio of volume to surface area). The line intensity is directly proportional to the volume V_c of a cloud (and therefore the mass M_c) if molecular clouds are gravitationally bound. In that case $\Delta v_c \propto (M_c/R_c)^{1/2} \propto R_c(\langle n_H \rangle)^{1/2}$, where R_c is the cloud diameter and $\langle n_H \rangle$ is the average density. Hence, $I_{CO} \propto T_{CO} N_c M_c/(\langle n_H \rangle)^{1/2}$, which is sensitive to mass if T_{CO} and $\langle n_H \rangle$ are approximately constant in all clouds. If the [C II] line were optically thin, the CO line optically thick and the [C II] and CO filling factors similar, the observed constant ratio of [C II] to CO line intensities would imply that CO excitation temperatures scale directly with C^+ column density and thus with UV energy density:

$$\frac{I_{[C\,II]}(\tau_{[C\,II]} < 1)}{I_{CO}(\tau_{CO} > 1)} = 6.6 \times 10^4 \frac{N_{C^+}[17.5]}{T_{CO}\,(K)\,\Delta v_c\,(5\ km\ s^{-1})}\,. \tag{B10}$$

This is the "extreme" view mentioned in § IV*f*. For $I_{[C\,II]}/I_{CO} = 4.4 \times 10^3$, $N_{C^+}[17.5] = 2.7 T_{CO}(40\ K)\Delta v_c(5\ km\ s^{-1})$.

V. RATIO OF [C II] TO CO LINES: BOTH LINES OPTICALLY THICK

If both lines are optically thick, the integrated line ratio is

$$\frac{I_{[C\,II]}(\tau_{[C\,II]} > 1)}{I_{CO}(\tau_{CO} > 1)} = 4.5 \times 10^3 \frac{91\ K/(e^{91\ K/T_{C^+}} - 1)}{T_{CO}}\,. \tag{B11}$$

With $I_{[C\,II]}/I_{CO} = 4.4 \times 10^3$ and $T_{C^+} \sim 200$–400 K, we find

$$\langle T_{CO} \rangle = \frac{93\ K}{e^{91\ K/T_{C^+}} - 1} \approx 160\text{–}360\ K \approx \langle T_{C^+} \rangle\,. \tag{B12}$$

With the exception of the Orion-Trapezium region, such values for $\langle T_{CO} \rangle$ are much higher than has been estimated for the gas temperatures in the CO–emitting regions in our galaxy. This further supports our argument that the 158 μm [C II] line is probably optically thin in most sources.

VI. IMPORTANCE OF [C II] AND CO COOLING

We now estimate the relative importance of [C II] and CO cooling. The total CO intensity, integrated over all rotational lines (ergs s^{-1} cm^{-2} sr^{-1}) is given by

$$I_{tot}(CO) = \sum_{J=1}^{\infty} \frac{h\nu_J}{4\pi} A_J \left(\frac{n_J}{n_{CO}}\right) \beta(\tau_J) N_{CO}\,, \tag{B13}$$

where A_J and n_J are the Einstein coefficient and population of the Jth rotational state, respectively. For the escape probability $\beta(\tau_J)$, we take $\beta(\tau_J) \sim (1 - e^{-3\tau_J})/3\tau_J$, as is derived for a plane-parellel cloud with a large velocity gradient. An upper bound to I_{tot} is obtained if trapping is not significant ($\beta \rightarrow 1$) and if each collision leads to photon emission (cf. McKee *et al.* 1982):

$$I_{tot}(CO) \sim 2 \times 10^{-5} N_{CO}[17.5] n_{H_2} (5 \times 10^3\ cm^{-3}) T_{CO}(40\ K); \tag{B14}$$

the ratio of total cooling of [C II] to CO is then

$$\frac{L_{[C\,II]}}{L_{CO}} = \frac{I_{[C\,II]}}{I_{tot}(CO)} \sim 60 \left[\frac{I_{[C\,II]}/I_{CO}(1 \rightarrow 0)}{4.4 \times 10^3}\right] \left(\frac{5 \times 10^3\ cm^{-3}}{n_{H_2}}\right) \left(\frac{40}{T_{CO}}\right)^2\,. \tag{B15}$$

Hence, if $T_{CO} < T_{C^+} \sim 300$ K and $n_{H_2} \lesssim 10^5\ cm^{-3}$, [C II] is one to two orders of magnitude more important than CO in cooling the surfaces of molecular clouds illuminated by intense UV radiation fields (assuming that the C^+ abundance is high). Only [O I] 63 μm is a better coolant than [C II] in photodissociation regions (TH).

REFERENCES

Bania, T. M. 1977, *Ap. J.*, **216**, 381.
Becklin, E. E., Gatley, I., Matthews, K., Neugebauer, G., Snellgren, K., Werner, M. W., and Wynn-Williams, C. G. 1980, *Ap. J.*, **236**, 441.
Blitz, L., and Shu, F. H. 1980, *Ap. J.*, **238**, 148.
Combes, F., Encrenaz, P. J., Lucas, R., and Weliachew, L. 1978, *Astr. Ap.*, **67**, L13.
Dalgarno, A., and McCray, R. M. 1972, *Ann. Rev. Astr. Ap.*, **10**, 375.
de Jong, T. 1977, *Astr. Ap.*, **55**, 137.
de Jong, T., Dalgarno, A., and Boland, W. 1980, *Astr. Ap.*, **91**, 68.
Ellis, H. B., and Werner, M. W. 1984, in preparation.
Emery, R. J., and Kessler, M. F. 1984, in *Galactic and Extragalactic Infrared Spectroscopy*, ed. M. F. Kessler and J. P. Phillips (Dordrecht: Reidel), p. 289.
Evans, N. J., II. 1981, in *IAU Symposium 96, Infrared Astronomy*, ed. C. G. Wynn-Williams and D. J. Cruikshank (Dordrecht: Reidel), p. 107.
Flaud, J.-M., Camy-Peyret, C., and Johns, J. W. C. 1983, *Canadian J. Phys.*, **61**, 1462.
Flower, D. R., and Launay, J. M. 1977, *J. Phys. B.* **10**, 3673.
Frerking, M. A., Langer, W. D., and Wilson, R. W. 1982, *Ap. J.*, **262**, 590.
Gatley, I., Becklin, E. E., Snellgren, K., and Werner, M. W. 1979, *Ap. J.*, **233**, 575.
Genzel, R., Crawford, M. K., Townes, C. H., and Watson, D. M. 1985, in preparation.
Gerola, H., and Glassgold, A. E. 1978, *Ap. J. Suppl.*, **37**, 1.
Glassgold, A. E., and Langer, W. D. 1975, *Ap. J.*, **197**, 347.
Güsten, R., Walmsley, C. M., and Pauls, T. 1981, *Astr. Ap.*, **103**, 197.
Haller, E. E., Hueschen, M. R., and Richards, P. L. 1979, *Appl. Phys. Letters*, **34**, 495.
Harper, D. A., Low, F. J., Rieke, G. H., and Thronson, H. A. 1976, *Ap. J.*, **205**, 136.
Harvey, P. M., Campbell, M. F., and Hoffman, W. F. 1977, *Ap. J.*, **211**, 786.
Harvey, P. M., Thronson, H. A., Jr., and Gatley, I. 1980, *Ap. J.*, **235**, 894.
Harwit, M. 1984, in *Galactic and Extragalactic Infrared Spectroscopy*, ed. M. F. Kessler and J. P. Phillips (Dordrecht: Reidel), p. 145.
Hildebrand, R. H. 1983, *Quart. J. R.A.S.*, **24**, 267.
Hyland, A. R., McGregor, P. J., Robinson, G., Thomas, J. A., Becklin, E. E., Gatley, I., and Werner, M. W. 1980, *Ap. J.*, **241**, 709.
Jaffe, D. T., Becklin, E. E., and Hildebrand, R. 1984, *Ap. J.* (*Letters*), **285**, L31.
Jaffe, D. T., Crawford, M. K., Genzel, R., Lugten, J. B., and Townes, C. H. 1985, in preparation.
Jaffe, D. T., and Pankonin, V. 1978, *Ap. J.*, **226**, 869.
Jura, M. 1978, in *Protostars and Planets*, ed. T. Gehrels (Tucson: University of Arizona Press), p. 165.
Knapp, G. R., Phillips, T. G., Huggins, P. J., Leighton, R. B., and Wannier, P. G. 1980, *Ap. J.*, **240**, 60.

Kurtz, N. L., Smyers, S. D., Russell, R. W., Harwit, M., and Melnick, G. 1983, *Ap. J.*, **264**, 538.
Lada, C. J., and Black, J. H. 1976, *Ap. J.* (*Letters*), **203**, L75.
Lada, C. J., Thronson, H. A., Jr., Smith, H. A., Harper, D. A., Keene, J., Loewenstein, R. F., and Smith, J. 1982, *Ap. J.* (*Letters*), **251**, L91.
Langer, W. 1976, *Ap. J.*, **206**, 699.
Launay, J.-M., and Roueff, E. 1977, *J. Phys.* B, **10**, 879.
Leighton, R. B. 1978, Final Tech. Rept., NSF Project AST 73-04708.
Liszt, H., and Burton, W. B. 1978, *Ap. J.*, **226**, 790.
Masson, C. R. 1982, *Astr. Ap.*, **114**, 270.
McKee, C. F., Storey, J. W. V., Watson, D. M., and Green, S. 1982, *Ap. J.*, **259**, 647.
Mebold, U., Winnberg, A., Kalberla, P. M. W., and Goss, W. M. 1982, *Astr. Ap.*, **115**, 223.
Mezger, P. G. 1978, *Astr. Ap.*, **70**, 565.
Milman, A. S., Knapp, G. R., Kerr, F. J., Knapp, S. L., and Wilson, W. J. 1975, *A.J.*, **80**, 93.
Morris, M., Polish, N., Zuckerman, B., and Kaifu, N. 1983, *A.J.*, **88**, 1228.
Morris, M., and Rickard, L. J. 1982, *Ann. Rev. Astr. Ap.*, **20**, 517.
Moseley, H. 1980, *Ap. J.*, **238**, 892.
Mufson, S. L., and Liszt, H. S. 1977, *Ap. J.*, **212**, 664.
Olofsson, H., and Rydbeck, G. 1984, preprint.
Osterbrock, D. E. 1974, *Astrophysics of Gaseous Nebulae* (San Francisco: Freeman).
Rickard, L. J., and Harvey, P. M. 1983, *Ap. J.* (*Letters*), **268**, L7.
———. 1984, preprint.
Rickard, L. J., Palmer, P., Morris, M., Turner, B. E., and Zuckerman, B. Z. 1977, *Ap. J.*, **213**, 673.
Rieke, G. H., and Lebofsky, M. J. 1979, *Ann. Rev. Astr. Ap.*, **17**, 477.
Rieke, G. H., Lebofsky, M. J., Thompson, R. J., Low, F. J., and Tokunaga, A. T. 1980, *Ap. J.*, **238**, 24.
Rogstad, D. H., Lockhart, I. A., and Wright, M. C. H. 1974, *Ap. J.*, **193**, 309.
Russell, R. W., Melnick, G., Gull, G. E., and Harwit, M. 1980, *Ap. J.* (*Letters*), **240**, L99.
Russell, R. W., Melnick, G., Smyers, S. D., Kurtz, N. T., Gosnell, T. R., Harwit, M., and Werner, M. W. 1981, *Ap. J.* (*Letters*), **250**, L35.
Sanders, D. B., Solomon, P. M., and Scoville, N. Z. 1984, *Ap. J.*, **276**, 182.
Sargent, A. I., Sutton, E. C., Masson, C. R., Lo, K. Y., and Phillips, T. G. 1984, preprint.
Schloerb, F. P., and Loren, R. B. 1982, *Ann. NY Acad. Sci.*, **395**, 32.
Scoville, N. Z., and Young, J. S. 1983, *Ap. J.*, **265**, 148.
Scoville, N. Z., Young, J. S., and Lucy, L. B. 1983, *Ap. J.*, **270**, 443.
Smith, J. 1982, *Ap. J.*, **261**, 463.
Solomon, P. M., and Snaders, D. B. 1980, in *Giant Molecular Clouds in the Galaxy*, ed. P. M. Solomon and M. G. Edwards (New York: Pegamon), p. 41.
Stacey, G. J., Viscuso, P. J., Fuller, C. E., and Kurtz, N. T. 1984, preprint.
Stark, A. A. 1982, in *Extragalactic Molecules*, ed. L. Blitz and M. Kutner (Green Bank: NRAO), p. 77.
Stark, A. A., and Carlson, E. R. 1984, *Ap. J.*, **279**, 122.
Storey, J. W. V., Watson, D. M., and Townes, C. H. 1980, *Internat. J. Infrared Millimeter Waves*, **1**, 15.
Storey, J. W. V., and Watson, D. M., Werner, M. W., and Crawford, M. K. 1985, in preparation.
Sutton, E. C., Masson, C. R., and Phillips, T. G. 1983, *Ap. J.* (*Letters*), **275**, L49.
Telesco, C. M., Becklin, E. E., Wynn-Williams, C. G., and Harper, D. A. 1984, *Ap. J.*, **282**, 427.
Telesco, C. M., and Harper, D. A. 1977, *Ap. J.*, **211**, 475.
———. 1980, *Ap. J.*, **235**, 392.
Tielens, A. G. G. M., and Hollenbach, D. 1984, in preparation (TH).
Ulich, B. L., and Haas, R. W. 1976, *Ap. J.* (*Suppl.*), **30**, 247.
Walmsley, C. M. 1975, in H II *Regions and Related Topics*, ed. T. L. Wilson and D. Downes (New York: Springer), 17.
Watson, D. M. 1984, in *Galactic and Extragalactic Infrared Spectroscopy*, ed. M. F. Kessler and J. P. Phillips (Dordrecht: Reidel), p. 195.
Watson, D. M., Crawford, M. K., Genzel, R., Lugten, J. B., and Townes, C. H. 1984*a*. in preparation.
Watson, D. M., Genzel, R., Townes, C. H., Werner, M. W., and Storey, J. W. V., 1984*b*, *Ap. J.* (*Letters*), **279**, L1.
Weliachew, L., Fomalont, E. B., and Greisen, E. W. 1984, preprint.
Werner, M. W. 1970, *Ap. Letters*, **6**, 81.
Woody, D. P., Miller, R. E., and Wengler, M. J. 1984, *IEEE-MTT*, submitted.
Young, J. S., and Scoville, N. Z. 1982, *Ap. J.*, **258**, 467.
———. 1984, preprint.

M. K. CRAWFORD, R. GENZEL, and C. H. TOWNES: Department of Physics, University of California, Berkeley, CA 94720

DAN M. WATSON: California Institute of Technology, Downs Laboratory of Physics, 320-47, Pasadena, CA 91125